National Aeronautics and Space Administration

Commercial Satellite Data Acquisition Program

Umbra Synthetic Aperture Radar Quality Assessment Report

Commercial Satellite Data Acquisition Program Umbra Synthetic Aperture Radar Quality Assessment Report

Signature/Approval Page

Approval by:

05/20/2026

Melissa Yang Martin
Commercial Satellite Data Acquisition Program Manager
Earth Science Division
Headquarters/NASA

Date

Accepted by:

05/20/2026

Dana Ostrenga
Commercial Satellite Data Acquisition Project Manager
Earth Science Division
GSFC/NASA

Date

Preface

This document is under CSDA Project configuration control. Once this document is approved, CSDA approved changes are handled in accordance with Class I and Class II change control requirements described in the CSDA Configuration Management Procedures based on NASA standard configuration practices, and changes to this document shall be made by document change notice (DCN), documented in the Change History Log or by complete revision.

Abstract

The evaluation summarized in this report was conducted by subject matter experts (SMEs) funded by NASA's Commercial Satellite Data Acquisition (CSDA) Program. The SMEs evaluated the radiometric and geometric quality of Umbra data for the NASA Earth science research and applications community. The results of the evaluation help to inform NASA program management on the quality of the data for NASA science.

Authored and prepared by

MinJeong Jo
SAR Quality Assessment Expert
University of Maryland, Baltimore County
National Aeronautics and Space Administration

Jordan Bell
CSDA SAR Subject Matter Expert
Marshall Space Flight Center
National Aeronautics and Space Administration

Jaime Nickeson
CSDA Technical Science Coordinator
Science Systems and Applications Inc
National Aeronautics and Space Administration

Frederick Policelli
CSDA Project Scientist
Goddard Space Flight Center
National Aeronautics and Space Administration

Change History Log

Revision	Effective Date	Description of Changes
1.0	04/30/2026	First reviewed version for public release

Table of Contents

List of Figures

List of Tables

Acronyms & Abbreviations

ALE	Absolute Location Error
ARD	Analysis Ready Data
ATBD	Algorithm Theoretical Basis Document
CF	Climate & Forecast (Metadata Convention)
CR	Corner Reflector
CEOS	Committee on Earth Observation Satellites
CPHD	Compensated Phase History Data
DOI	Digital Object Identifier
EDAP	Earthnet Data Assessment Project
ESA	European Space Agency
FAIR	Findable, Accessible, Interoperable and Reusable
FRM	Fiducial Reference Measurement
GEC	Geo Ellipsoid Corrected
GUM	Guide to the Expression of Uncertainty in Measurement
HH	Sensor polarization: Horizontal transmit, Horizontal receive
INSPIRE	Infrastructure for Spatial Information in Europe
IRF	Impulse Response Function
ISLR	Integrated Side Lobe Ratio
ISRO	Indian Space Research Organization
NESZ	Noise Equivalent Sigma Zero
NetCDF	Network Common Data Format
NISAR	NASA-ISRO Synthetic Aperture Radar
NITF	National Imagery Transmission Format
PSLR	Peak Side Lobe Ratio
PUG	Product User Guide
PUM	Product User Manual
QA	Quality Assessment
RCS	Radar Cross Section
SAR	Synthetic Aperture Radar
SI	Système International (International System of Units)
SICD	Sensor Independent Complex Data
SIDD	Sensor Independent Derived Data
SLC	Single-look Complex
STAC	Spatio-Temporal Asset Catalog
URL	Universal Resource Locator
VV	Sensor Polarization: Vertical transmit, Vertical receive

Executive Summary

The Commercial Satellite Data Acquisition (CSDA) Program was established to identify, evaluate, and acquire data from commercial sources that support the National Aeronautics and Space Administration (NASA) Earth science research and application goals. NASA's Earth Science Division (ESD) recognizes the potential impact commercial satellite constellations may have in encouraging/enabling efficient approaches to advancing Earth System Science and applications development for societal benefit. Commercially acquired data may also provide a cost-effective means to augment and/or complement the suite of Earth observations acquired by NASA and other U.S. government agencies and those by international partners and agencies.

In this report, CSDA provides an evaluation of the quality of data provided by the Umbra X-band Synthetic Aperture Radar (SAR) satellite constellation for advancing NASA's Earth system science research and applications. This evaluation of Umbra radiometric and geometric performance was carried out by NASA subject matter experts (SMEs) that were enlisted to evaluate the fundamental quality of the Umbra data following the Joint NASA/European Space Agency (ESA) assessment guidelines (ESA-NASA, 2024).

Data from the Umbra constellation of satellites included archive data from satellites that were no longer operational during the evaluation period. All data products delivered were processed using Umbra processor versions 4.23.0 to 4.24.0. Details about an assessment performed by a group of selected principal investigators on the utility of Umbra data for NASA science is available in a separate report, the *Commercial Satellite Data Acquisition Program Umbra Principal Investigator Evaluation Summary.*

Umbra has a Product User Guide available online that was heavily referenced for this assessment. Product details in the metadata were provided in the common Spatio-Temporal Asset Catalog (STAC) format. The product information provided in the vendor documentation guides and the product metadata together provide adequate information to work with the data. This information provided a characterization of the SAR system and data, together with the metadata and ancillary information. Additional documentation provided to CSDA by the vendor are not public, including limited pre- and post-flight calibration information. Metrological traceability documentation was not provided.

The quality assessment was mainly performed on the single-look complex (SLC) Level 1 data products provided by Umbra in Sensor Independent Complex Data (SICD) format, a standardized specification for SLC data developed and maintained by the US National Geospatial-Intelligence Agency (NGA). Additional Level 2 products were also used in science usability assessments by the evaluation team. The uncertainty values relevant for SAR (i.e. noise equivalent sigma zero [NESZ]) are provided at the product level in the metadata. Radiometric parameters for each product are provided in the metadata to convert the observed radar brightness to meaningful units (i.e. $sigma_0$). The vendor provided documentation does not contain information on how the performance values are derived.

This report provides results of an independent study of the Umbra SAR essential quality parameters, such as spatial resolution, PSLR, ISLR, geolocation accuracy, absolute radiometric

accuracy, radiometric stability, and radiometric sensitivity (NESZ). Representative datasets were collected by Umbra over various calibration test sites, including distributed and point targets. Data analysis was performed on data collected in Spotlight (SP) mode. The validation by the CSDA SAR SME team was performed using multiple software packages, including code developed internally at NASA Goddard Space Flight Center (GSFC) as well as the commercial GAMMA Remote Sensing SAR data processing package.

On the geometric side, our assessment found that for spatial resolution, the quality analysis results agreed with specifications provided by Umbra. The measured ground-range resolution was slightly larger than the expected resolution, with ratios ranging from 1.04 to 1.27. In contrast, the measured azimuth resolution was generally finer than the expected resolution, with ratios ranging from 0.78 to 0.96. The measured PSLR and ISLR values ranged from -14 to -19 dB and -13 to -20 dB, respectively, which were generally close to the expected theoretical values. The quality analysis results for geolocation accuracy, however, were not universally in agreement with the specifications indicated by Umbra, with an absolute location error (ALE) of approximately 16.37 m ± 13.56 m. Based on the available Umbra documentation, and our independent assessment, we conclude that the overall geometric performance of the Umbra data is of basic quality, due in part to the fact that the geolocation was out of specification, but also because at times it was significantly so.

The Umbra radiometric performance, which was assessed in terms of absolute accuracy, stability, and sensitivity, was found to underperform relative to that of well-calibrated reference SAR systems. Most images also show noticeable $sigma_0$ variation across the swath, suggesting that antenna pattern effects may not have been fully compensated during radiometric calibration.

1. Cal/Val Maturity Matrices

1.1. Summary Cal/Val Maturity Matrix

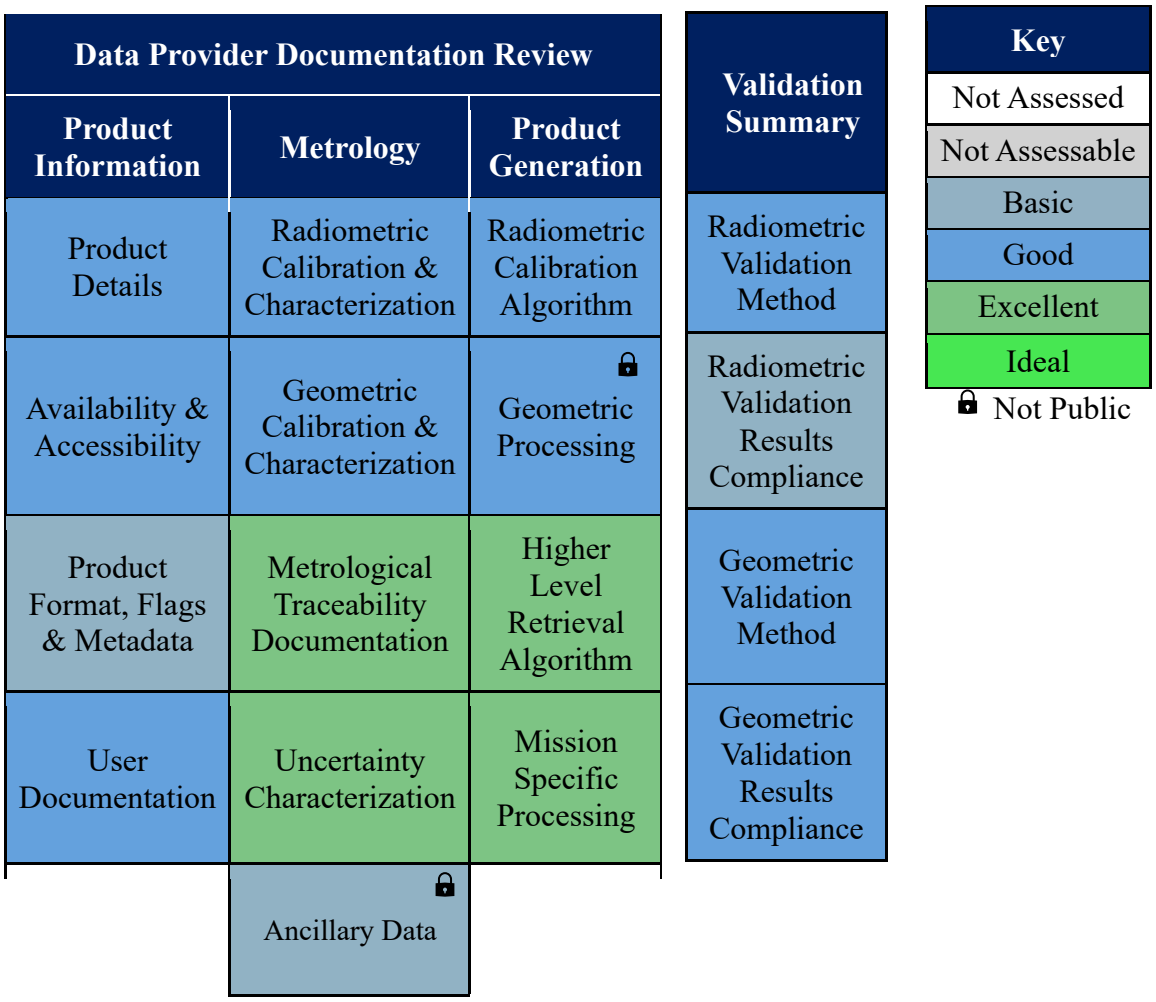

Figure 1. Summary Cal/Val Maturity Matrix for Umbra.

1.2. Detailed Validation Maturity Matrix

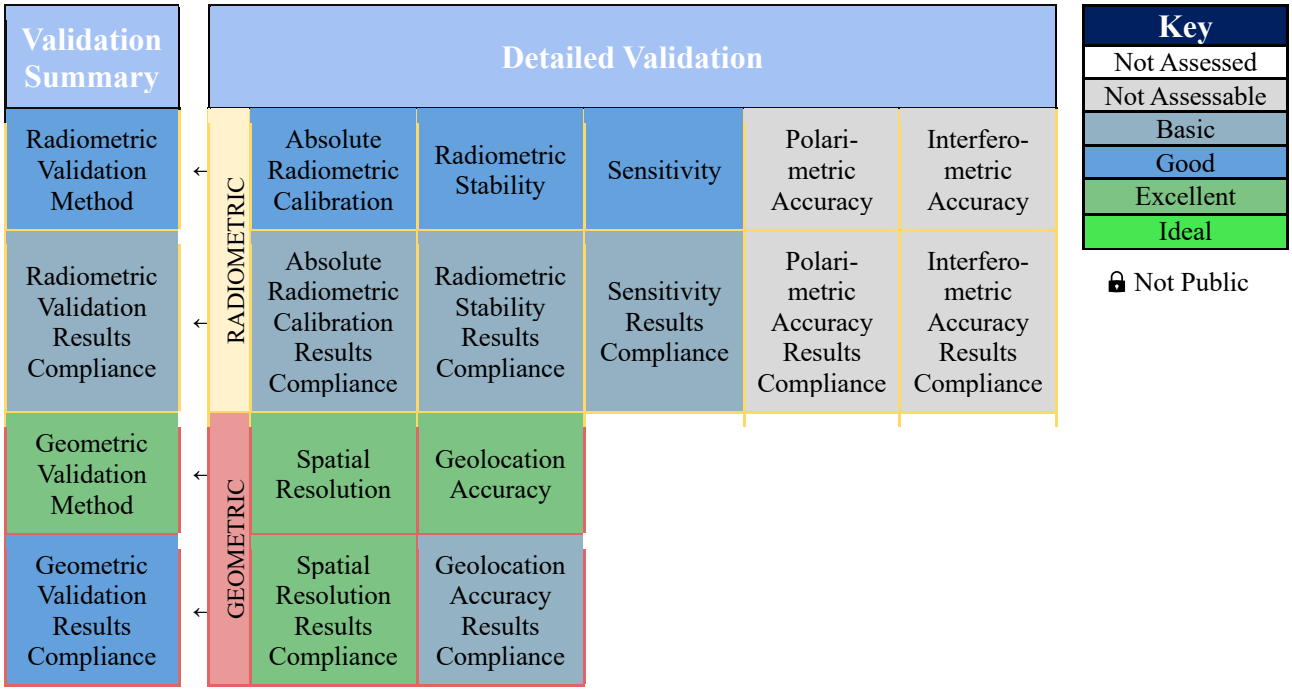

Figure 2. Detailed Validation Maturity Matrix for the SAR domain, showing the Validation Summary column from the Summary Validation Maturity Matrix.

2. Data Provider Documentation Review

2.1. Product Information

Product Details	
Good	
Justification	Robust description of products and associated metadata. Data such as temporal extent, spatial extent, and number of active satellites is not explicit in vendor-provided top-level documentation but can be determined through metadata catalog.
Product Name	2025-12-25-04-14-33_UMBRA-09_MM YYYY-MM-DD-HH-MM-SS_UMBRA-XX_MM YYYY = Acquisition Year MM = Acquisition Month DD = Acquisition Day HH = Acquisition Hour MM = Acquisition Minute SS = Acquisition Second UMBRA-XX = Collector Name MM = Product Type
Sensor Name	Umbra-SAR
Sensor Type	X-band SAR
Mission Type	Commercial Earth Observation
Mission Orbit	Sun Synchronous
Product Version Number	Umbra SAR Processor 4.23.0 - 4.24.0
Product ID	A string of digits and letters (unique for each product) e.g.: "collect_id": "61483b2a-0993-4aa0-afaa-d4a9e9154187"
Processing level of Product	Level 0 (CPHD) Level 1 (SICD) Level 2 (SIDD, GEC)
Measured Quantity Name	Radar backscatter, Beta Nought, Gamma Nought, Sigma Nought, and Radar Cross Section.
Measured Quantity Units	Radar brightness β_0 and normalized radar cross section σ_0 are unitless quantities representing reflectivity per unit area.
Stated Measurement Quality	Absolute Geolocation Accuracy is stated at 8 m. Theoretical NESZ provided in the metadata.
Spatial Resolution	Umbra's primary imaging mode is Spotlight, with spatial resolutions ranging from 0.25 m to 1 m. Umbra introduced a Scan mode during the 1-year evaluation which can vary in spatial resolutions of 0.5 m, 1 m, or 2 m.
Spatial Coverage	The standard Spotlight scene size is 5 km x 5 km. The scan mode scenes can have lengths between 25 and 100 km depending on spatial resolution and is 8 km wide.

Temporal Resolution	Umbra's orbit is 7-day repeat. Multiple satellite sub-daily revisit.
Temporal Coverage	Umbra's first satellite was launched in June 2021. By August 2024, Umbra had launched its 10th satellite in the constellation.
Point of Contact	Omar Wheatley: omar.wheatley@umbraspace.com Nolan Anderson: nolan.anderson@umbraspace.com
Product Locator (DOI/URL)	N/A
Conditions for Access and Use	All data used in this evaluation were purchased by CSDA under U.S. Government-wide license. Licenses can be found on the CSDA website (https://science.nasa.gov/earth-science/csda).
Limitations on Public Access	N/A
Product Abstract	N/A

Availability & Accessibility	
Grade: Good	
Justification	Umbra data meets 11/14 of the FAIR principals. The unfulfilled principles are: F1: (Meta)data are assigned a globally unique and persistent identifier F4: (Meta)data are registered or indexed in searchable resource I3: (Meta)data include qualified references to other (meta)data
Compliant with FAIR principles	78%
Data Management Plan	The vendor does not appear to have a data management plan.
Availability Status	Data is available to customers through a vendor provided API and web portal

Product Format	
Grade: Good	
Justification	The most common product types are provided in CPHD, SICD, SIDD, Geocoded Ellipsoid Corrected (GEC) formats. CPHD comes in CPHD format, SICD and SIDD types come in the NITF format, and the GEC product is delivered in a GeoTiff format. Umbra offers additional products in varying formats, but those products were not a part of this assessment. The default metadata for all products is STAC.
Product File Format	GeoTiff, NITF
Metadata Conventions	STAC
Analysis Ready Data?	No

User Documentation		
Grade: Basic		
Justification	The online Umbra Product guide is the only documentation that was provided by the vendor that is publicly available. Additional internal documentation was provided by the Vendor to the authors of this report for review. No specific ATBD was provided.	
Document	***Reference***	
Product User Guide	*Umbra Product Guide (Umbra, 2025)*	
ATBD	N/A	

2.2. Metrology

Radiometric Calibration & Characterization	
Grade: Good	
Justification	Vendor provides calibration coefficients for Sigma, Gamma, Beta, and RCS as tags within the GEC GeoTiff product. Vendor does not appear to provide peak estimates of NESZ within GeoTiff tags or STAC metadata.
References	• *Umbra Product Guide (Umbra, 2025)*

Geometric Calibration & Characterization	
Grade: Good	
Justification	Vendor acknowledges that absolute geolocation accuracy is 8 meters. Additional details about calibration locations and activities are provided to CSDA SME Team.
References	• *Umbra Product Guide (Umbra, 2025)* • *Umbra Calibration Activity (Proprietary, 2026)*

Metrological Traceability Documentation	
Grade: Not Assessable	
Justification	The evaluation team did not have access to metrological traceability documentation.
References	N/A

Uncertainty Characterization	
Grade: Not Assessable	
Justification	Vendor-provided data products do not appear to contain Guide to the Expression of Uncertainty in Measurement (GUM, JCGM 2008)-compliant uncertainty metrics.
References	N/A

Ancillary Data	
Grade: Basic	
Justification	The vendor-provided internal documentation does note the use of ancillary data in the formulation of products, though the information is incomplete. The public facing product guide does not denote any ancillary information.
References	• *Umbra Product Formation (Proprietary, 2026)* • *Umbra Product Guide (Umbra, 2025)*

2.3. Product Generation

Radiometric Calibration Algorithm	
Grade: Good	
Justification	Basic image format generation is provided publicly by vendor in product guide for different file formats that are offered. Vendor provided additional internal documentation on radiometric calibration activities.
References	• *Umbra Product Guide (Umbra, 2025)* • *Umbra Calibration Activity (Proprietary, 2026)*

Geometric Processing	
Grade: Good	
Justification	Geometric processing, especially for the GEC product, are described at a basic level in the vendor's product guide. Internal documentation provided by the vendor describes non-technical geometric calibration activities
References	• *Umbra Product Guide (Umbra, 2025)* • *Umbra Product Formation (Proprietary, 2026)*

Higher Level Retrieval Algorithm	
Grade: Not Assessable	
Justification	There were no higher-level data products evaluated.
References	N/A

Mission-Specific Processing	
Grade: Not Assessable	
Justification	There was no mission specific processing performed on the Umbra products.
Reference	N/A

3. Detailed Validation – Radiometric

This section presents the detailed measurement validation, such as the absolute radiometric accuracy, radiometric stability, and sensitivity assessments conducted with the Umbra dataset. Sensor Independent Complex Data (SICD), a standardized specification for SAR data developed and maintained by the US National Geospatial-Intelligence Agency (NGA), was used for the evaluation.

For the radiometric analyses, the sigma$_0$ was calculated as follows (NGA, 2023):

$$\sigma^0(x_{row}, y_{col}) = \text{SigmaZero\_SF}(x_{row}, y_{col}) \cdot \text{P}(x_{row}, y_{col}) \quad (1)$$

The scale factor is represented as a two-dimensional polynomial of image coordinates:

$$\text{SigmaZero\_SF}(x_{row}, y_{col}) = \sum_{m=0}^{M_{SIG}} \sum_{n=0}^{N_{SIG}} c_{SIG}(m,n)\,(x_{row})^m (y_{col})^n \quad (2)$$

Here, $c_{SIG}(m,n)$ are polynomial coefficients, and M_{SIG}, N_{SIG} define the polynomial orders in the row and column directions. The resulting sigma$_0$ values were then converted to the dB scale:

$$\sigma^0_{dB} = 10\,log10\,(\,\sigma^0) \quad (3)$$

where SigmaZero_SF denotes radiometric scaling factor, and *P* is the pixel power value, sometimes referred to as the pixel intensity. This analysis included data from the Umbra constellation as shown in Table 1, and a detailed list of all individual scenes used in the radiometric assessment are provided in Appendix Table A1.

Table 1. Summarized list of Umbra data used for the radiometric assessment. A detailed list of the parameters for individual satellite scenes used in the assessment is available in Appendix A, Table A1.

Test Area	Number of Scenes	Acquisition Date	Satellite Number	Imaging Mode	Polarization	Incidence Angle
Rosamond	9	08/17/2024 - 09/12/2024	4, 5, 6, 7, 8	Spotlight	VV	32.26 – 54.55
Doldrums	2	08/29/2025 – 09/01/2025	5	Spotlight	VV	25.47 – 34.31
	38	08/16/2025 – 09/11/2025	5, 8, 9, 10	Spotlight	HH	15.39 – 34.15
Amazon	4	09/01/2025 – 09/09/2025	8, 10	Spotlight	VV	29.2 – 34.39
	36	08/27/2025 – 09/09/2025	5, 8, 9, 10	Spotlight	HH	17.33 – 34.89

We used archived data for the radiometric assessment of point targets at Rosamond. To ensure consistency, images with similar acquisition geometry (e.g., orbit, incidence angle, and spatial resolution) were selected. Among the available datasets, the VV-polarization image stack was the most suitable for obtaining a sufficient number of images for statistical analysis.

The Amazon rainforest regions are widely used as a homogeneous distributed target for assessing SAR radiometric accuracy and stability because large areas of dense tropical forest exhibit relatively uniform backscatter at the spatial scales of typical satellite products. This spatial homogeneity, combined with broad geographic extent and frequent repeat coverage, enables robust statistical evaluation of radiometric performance by examining mean backscatter levels and temporal variability across multiple acquisitions. Figure 3 shows the Amazon rainforest locations where Umbra images were collected for the radiometric accuracy and stability evaluation.

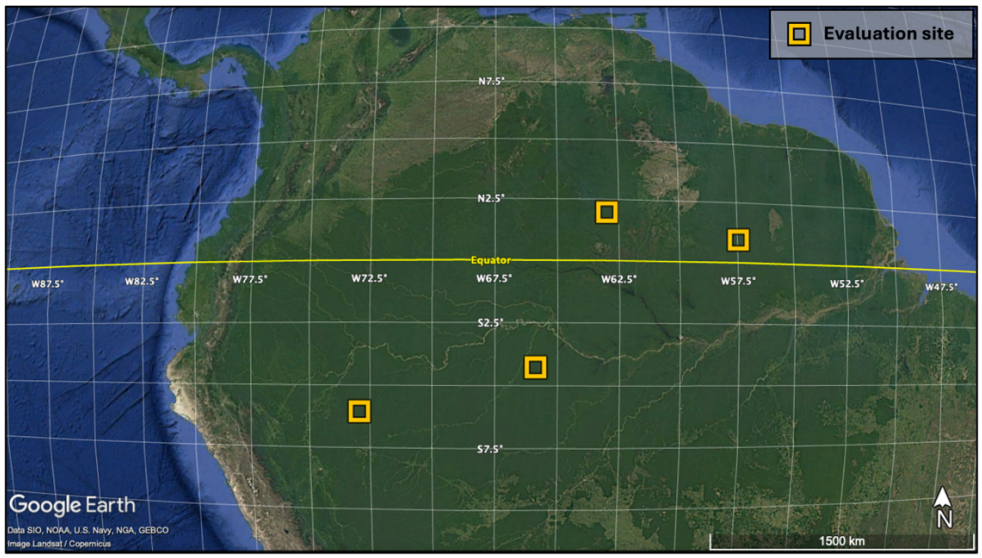

Figure 3. A Google Earth overview of the Amazon rainforest sites. The rectangles show the locations where Umbra images were collected.

The Doldrums of the Atlantic and Pacific equatorial regions serve as essential low-signal calibration sites for assessing the radiometric sensitivity and Noise Equivalent Sigma Zero (NESZ) of SAR sensors. These equatorial regions are characterized by exceptionally low wind speeds and minimal wave action, producing images with extremely low backscatter (σ^0). Figure 4 shows the locations where Umbra images were acquired for the evaluation.

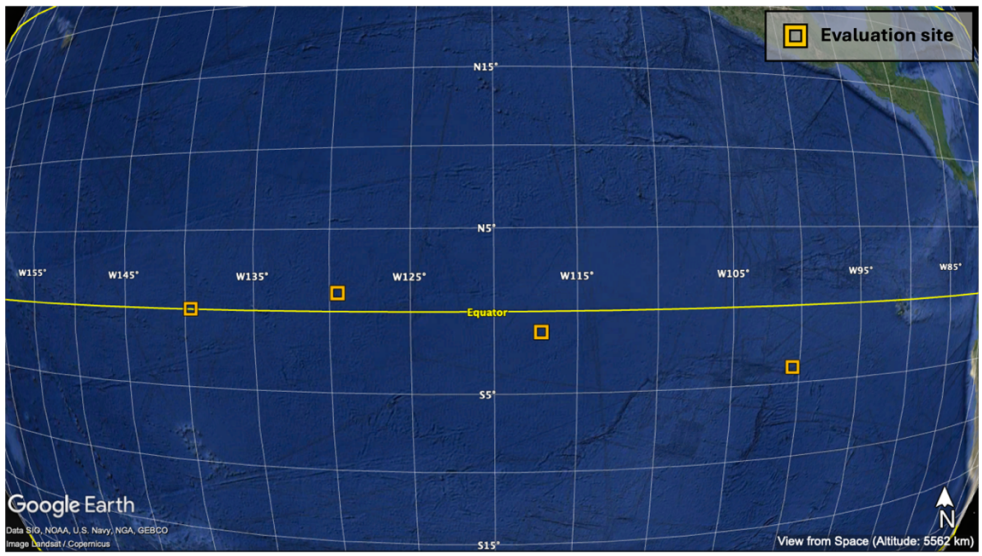

Figure 2. A Google Earth overview of the Doldrums sites. The rectangles show the locations where Umbra images were collected for radiometric sensitivity and NESZ assessment.

3.1. Absolute Radiometric Calibration

3.1.1. Method

The absolute radiometric accuracy of the imagery was validated using scenes over the Amazon rainforest and the Rosamond corner reflector array (RCRA) calibration site. The Amazon rainforest was used as a distributed target under the assumption that it represents a uniform and invariant target across the swath. It is also assumed that the uncertainty in measurement of the $sigma_0$ is zero (i.e., speckle is ignored). For a point target, such as the corner reflectors (CRs) at Rosamond, the absolute radiometric accuracy measures the uncertainty in measurement of the radar cross section (RCS) considering an invariant and well-known ground target.

Absolute radiometric accuracy was evaluated using calibrated $sigma_0$ values derived from the SICD products. Prior to analysis, pixels outside the valid data region were excluded using the *ValidData* polygon provided in the SICD metadata. The polygon vertices, defined in geographic coordinates (latitude and longitude), were used to generate a mask to ensure that only valid image areas were included in the assessment. Figure 5 shows an example of the original and the masked image used for the evaluation. Digital number (DN) values were then converted to $sigma_0$ using the *SigmaZeroSFPoly* calibration polynomial provided in the SICD metadata. The $sigma_0$ is derived from equations (1)-(3).

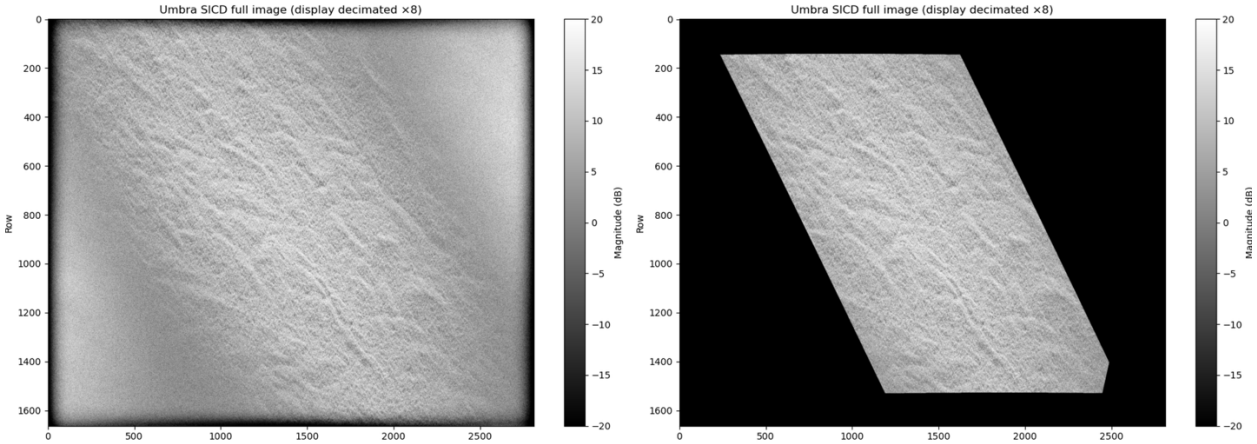

Figure 5. Example of valid data masking applied prior to radiometric analysis. The left panel shows the original SICD image, while the right panel shows the image after masking pixels outside the ValidData polygon defined in the SICD metadata. Only pixels within the valid data region were used for the absolute radiometric accuracy assessment.

For the point target, the expected $sigma_0$ was calculated from the theoretical RCS of the corner reflector at the corresponding incidence angle. The theoretical RCS of corner reflectors and related practical consideration were referenced from Sandia National Laboratories (Doerry, 2014). The absolute radiometric error was then calculated as the difference between the measured and expected $sigma_0$ values.

3.1.2. Results Compliance

The expected sigma0 value over a tree covered surface at X-band HH- and VV-polarization, for incidence angles between 13.5 and 35.5 degrees, is about -9.8 dB for both polarizations (Ulaby et al., 2019). The calibrated Umbra sigma0 values over sites in the Amazon have a mean value of -10.9 dB with a standard deviation of 1.8 dB, corresponding to an offset of approximately -1.1 dB relative to the literature-based expectation.

However, several images exhibited a noticeable variation in sigma0 as a function of incidence angle, characterized by a bell-shaped profile across the swath (Figure 6). This variation suggests that antenna pattern effects may not have been fully compensated during radiometric calibration. When antenna pattern correction is properly applied during radiometric calibration, the sigma0 distribution is expected to be relatively uniform across the incidence angle range (from near-range to far-range). As can be seen in Figure 6, only one image, which is inside the dotted box, displayed a nearly flattened $sigma_0$ profile, while most images still showed a residual variation with incidence angle.

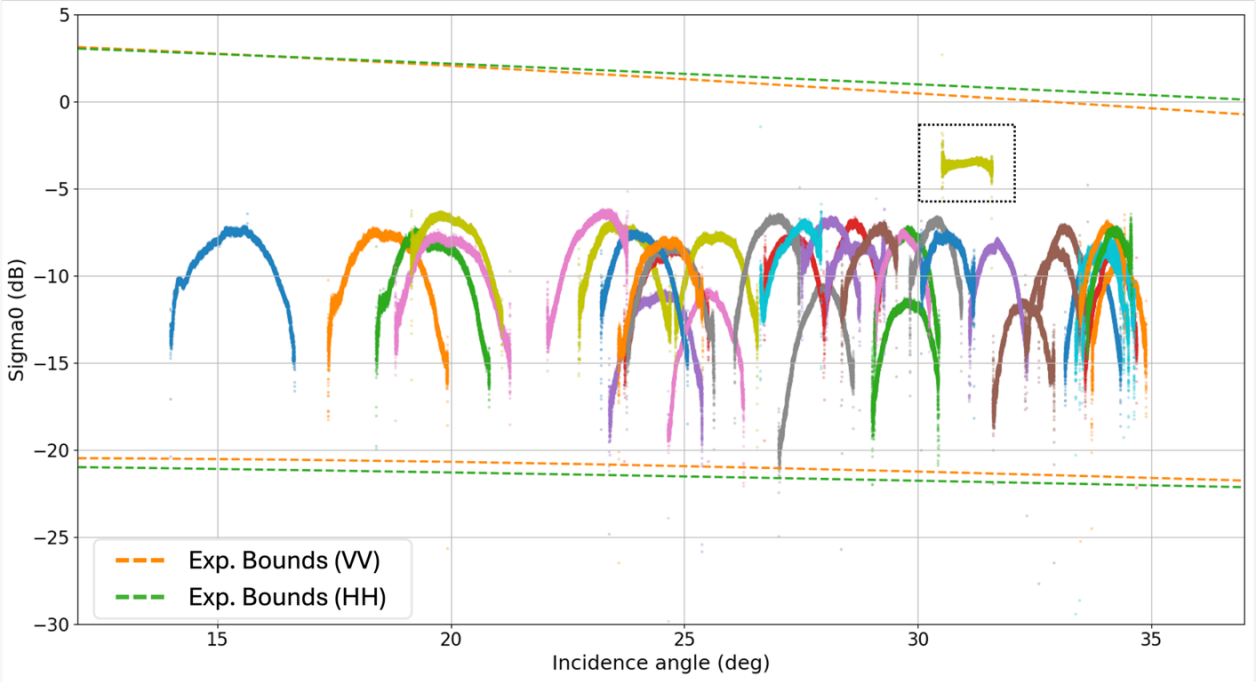

Figure 6. $Sigma_0$ values observed across a swath over various sites in the Amazon indicate that most of the scenes fall within the expected range. The dashed green and orange lines mark the +/- 3-sigma values for the expected range of X-band VV and HH $sigma_0$ values, per (Ulaby et al., 2019), respectively. However, most images exhibit a bell-shaped variation in $sigma_0$ across the swath, indicating residual antenna pattern effects that are not fully compensated.

The RCRA array consists of 0.7 m, 2.4 m and 4.8 m trihedral CRs and as well as two square-trihedral CRs (Table 2). CSDA acquired a set of 9 ascending, left-looking, VV-polarization images of the array from Umbra 04, 05, 06, 07, and 08 satellites from the Umbra archive for this analysis.

Table 2. Absolute calibration and radiometric stability result over Rosamond, CA corner reflector test site.

CR ID	CR Size (m)	Observed (dB)		Absolute Error (dB)	
		Mean	Std	Mean	Std
31	0.7	40.567	1.441	-0.788	2.293
33	0.7	40.403	1.884	-0.176	3.340
28	0.8	46.463	2.829	-7.382	3.425
34	0.8	50.368	2.259	-0.523	4.672
13	2.4384	52.917	1.545	-10.654	1.701
14	2.4384	52.550	2.568	-10.611	2.190
15	2.4384	56.596	1.551	-6.478	1.305
16	2.4384	53.895	3.844	-9.778	3.662
17	2.3989	57.274	1.141	-6.332	1.141
18	2.4384	48.311	4.259	-15.358	4.317
19	2.4384	58.408	1.065	-4.681	0.700
20	2.4384	55.231	2.531	-8.381	2.263
21	2.4384	46.401	2.586	-17.210	2.551
23	4.8	58.063	2.038	-15.900	3.368
24	4.8	57.204	2.812	-16.787	4.163
25	4.8	55.697	2.445	-18.311	3.873
26	4.8	57.810	3.150	-16.213	4.320
27	4.8	55.663	3.042	-18.363	4.467

The 0.7 m and 0.8 m corner reflectors are most suitable for high-resolution X-band sensors compared to the 2.4 m and 4.8 m corner reflectors. The 0.7 m and 0.8 m CRs have a mean absolute radiometric error of -3.9 dB and -0.48 dB, respectively. The 2.4 m and 4.8 m reflectors are better suited for L- and P-band sensors and show mean absolute errors of -9.94 and -17.11 dB, respectively (Table 2).

3.2. Radiometric Stability

3.2.1. Method

Radiometric stability was evaluated by repeatedly measuring signal consistency over two reference targets: the Amazon rainforest and the Rosamond calibration site. The Amazon rainforest was treated as a spatially uniform distributed target since its radar response is stable and expected to vary minimally over time. This is useful for assessing radiometric stability across the image swath.

The Rosamond site includes corner reflectors, which provide strong and well-defined returns and therefore serve as reliable reference points. Radiometric stability using corner reflectors was quantified by comparing repeated, independent measurements of the target reflectivity ($sigma_0$) across multiple acquisitions. This target can be located anywhere within the system dynamic range and swath, assuming that the uncertainty in measurement is negligible, and speckle noise is ignored.

3.2.2. Results Compliance

The expected variation of $sigma_0$ value over tree-covered surfaces within the X-band for VV- and HH-polarizations, and incidence angles between 17.33 and 34.89 degrees, is about 3.4 dB and 3.7 dB respectively. As shown in Figure 6, images with bell-shaped $sigma_0$ profiles, which likely indicate incomplete radiometric calibration, have a mean $sigma_0$ of -10 dB and a standard deviation of 1.8 dB for Spotlight (SP) mode imagery. Although Ulaby et al. (2019) provides expected ranges of $sigma_0$ variation for tree-covered surfaces, these values represent theoretical or empirical bounds. Compared to well-calibrated SAR systems (Schmidt et al., 2021), which typically exhibit sub-dB temporal variability under consistent conditions, the observed standard deviation of 1.8 dB indicates basic radiometric stability. In addition, as described in the previous section, most images show noticeable $sigma_0$ variation across the swath, suggesting that antenna pattern effects may not have been fully compensated during radiometric calibration.

Over the RCRA, there are three trihedral corner reflector sizes and one square-trihedral corner reflector size. Umbra data acquired over the 0.7 m corner reflectors have a radiometric variability of 1.4 to 1.9 dB, while the data from the 2.4 m and 4.8 corner reflectors have a radiometric variability of 1.1 to 4.3 dB and 2.0 to 3.2 dB respectively (Table 2). The radiometric variability of the data over the 0.8 square trihedra corner reflectors is 2.3 to 2.8 dB.

Mature, well-calibrated SAR missions typically exhibit sub-dB temporal variability in point-target observations (ESA, 2015; Schwerdt et al., 2018). In contrast, our analysis of corner reflectors at the Rosamond site indicates a temporal variability of approximately 1-3 dB across corner reflectors of different sizes. This level of variability is higher than that those reported for well-calibrated reference SAR systems, suggesting that the radiometric stability of the dataset underperforms against community standards for scientific analyses.

3.3. Sensitivity Validation

3.3.1. Method

The NESZ is estimated using signal-free regions (e.g., over very low or null backscatter targets, such as calm water or deserts) in the radar imagery. For this assessment, Umbra images were collected over regions of the Doldrums as they often provide near-zero wind conditions and correspondingly weak radar backscatter. Wind conditions at the time of each acquisition were obtained from the near-surface (2 m above ellipsoid) wind estimates from the Modern-Era Retrospective Analysis for Research and Applications, Version 2 (MERRA-2) reanalysis (Gelaro et al., 2017) to ensure that the observations used were from typically calm days. Two wind-speed regimes were evaluated, including typically calm cases (wind speed < 2 m/s) and moderately calm conditions (wind speed < 4m/s), to examine sensitivity performance under both low-wind scenarios. Expected $sigma_0$ values were then computed using a geophysical model function, using the XMOD2 model (Li & Lehner, 2013).

3.3.2. Results Compliance

Umbra theoretical NESZ values are reported in the metadata of each SICD product and typically range from approximately -22 to -15 dB. The specific NESZ values provided in the metadata are shown in Figure 7 as solid green lines. Figure 7 also presents the observed $sigma_0$ values from the Spotlight products as a function of incidence angle. The scenes collected for this assessment are listed in Table A1. To analyze $sigma_0$ values over ocean surface under calm to moderately calm conditions, we plotted only the images acquired on days with wind speeds below the threshold of 4 m/s (Fig 7).

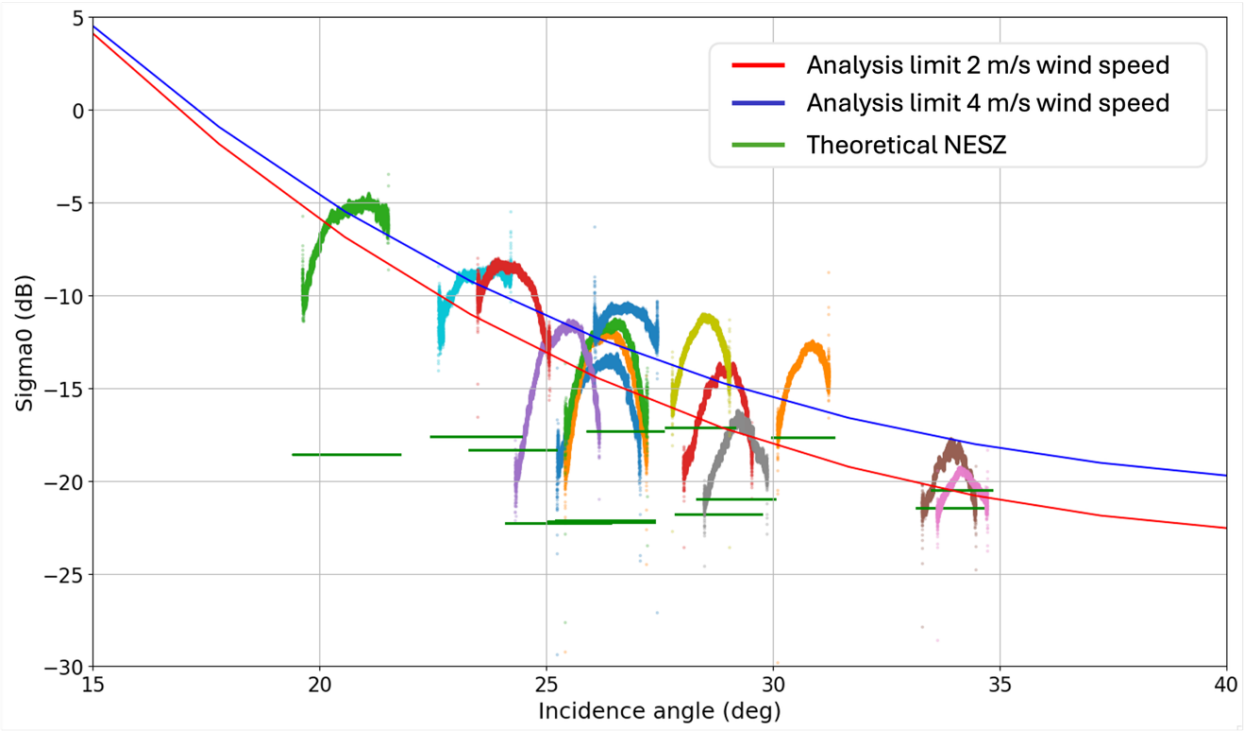

Figure 7. Noise Equivalent Sigma Zero (NESZ) as observed over the Doldrums. The solid red and blue lines indicate the XMOD2 calculated $sigma_0$ for a 2 m/s and a 4 m/s wind speed, respectively, at Umbra center frequency of 9.65 GHz. The curvature in $sigma_0$ along the range direction of the images may indicate that antenna pattern correction was either not applied or did not fully compensate.

In Figure 7, the solid red and blue lines represent the expected $sigma_0$ values assuming wind speeds of 2 m/s and 4 m/s, respectively. Wind speeds were estimated using MERRA-2 reanalysis data close to the Umbra acquisition time, and scenes acquired under wind conditions exceeding 4 m/s were excluded from the analysis. The observed $sigma_0$ values (colored dots) are generally above the theoretical NESZ and approach the expected values near an incidence angle approaching 34-degrees. As shown in Figure 7, for most analyzed images, the $sigma_0$ values fall below the analysis limit across the full incidence angle range, indicating that the observed $sigma_0$ values are dominated by system noise and the signal can be indistinguishable from noise. This suggests that the measurements may be approaching the sensor's sensitivity limit, preventing reliable estimation of NESZ values even under low-wind conditions. Additionally, the curvature in $sigma_0$ along the range direction of the images may indicate that antenna pattern correction was either not applied or did not fully compensate.

4. Detailed Validation – Geometric

This section describes detailed information of the impulse response function (IRF) quality assessment using point target analysis tools provided in GAMMA Remote Sensing software, in terms of spatial resolution, Peak Sidelobe Ratio (PSLR), Integrated Sidelobe Ratio (ISLR), and geolocation accuracy. The spatial resolution in radar coordinates was measured using the -3 dB width of the IRF in azimuth and range directions. The test datasets consisted of Umbra Spotlight (SP) mode imagery provided as SICD standard files. Table 3 lists the Umbra scenes used for the IRF quality assessment, showing test areas, satellite numbers, imaging mode, acquisition date range, and incidence angles. A detailed list of all individual scenes used for the geometric analysis are provided in Appendix Table A2.

Table 3. Summarized list of Umbra data used for geometric assessment. A detailed list of the parameters for individual satellite scenes used in the assessment is available in Appendix A, Table A2.

Test Area	Number of Scenes	Acquisition Date	Satellite Number	Imaging Mode	Target Res[m]	Incidence Angle
Rosamond	2	08/18/2024 - 09/02/2024	8	SP	0.16	53.06 – 53.08
	22	01/11/2024 – 10/04/2024	4, 5, 6, 7, 8	SP	0.25	32.13 – 54.55
	2	01/03/2024 – 01/04/2024	4, 6	SP	0.35	39.60 – 48.78
	25	10/09/2024 – 10/05/2025	5, 8, 9, 10	SP	0.5	18.91 – 79.46
	12	11/23/2024 – 10/02/2025	5, 8, 9, 10	SP	1	16.66 – 57.52
Oklahoma	13	09/05/2025 – 09/11/2025	5, 8, 9, 10	SP	0.35	25.28 – 39.56
	11	09/25/2025 – 09/30/2025	5, 8, 9, 10	SP	0.5	16.56 – 45.88
	9	09/24/2025 – 09/29/2025	5, 8, 9, 10	SP	1	26.14 – 55.93

The IRF analysis was performed over dedicated calibration sites with installed trihedral corner reflectors (CRs). The calibration sites used in this study include the RCRA in Rosamond, CA, and the Oklahoma Calibration Array created for a joint NASA mission with ISRO, India's Space Agency. This mission, the NASA-ISRO SAR (NISAR) satellite, created a NISAR Oklahoma Calibration Array that is distributed across a large area in western Oklahoma. There were 63 Umbra Spotlight scenes acquired for the Rosamond sites, and 33 acquired for the Oklahoma sites.

The Rosamond array is located near the south end of the Rosamond dry lakebed in the desert of southern California (Fig. 8). The array consists of 38 triangular trihedral CRs in 3 sizes and oriented east or west, as depicted in Figure 8. Five 4.8 meter and five 0.7 m CRs are oriented mostly eastward with an azimuth heading of 350°. The remaining five 0.7 m CRs have a heading angle of 90°. Of the twenty-three 2.4 m CRs, ten face mostly east, while the remaining thirteen are oriented west with an azimuth heading of 170°. Table 4 lists all the CRs installed at the Rosamond site. The coordinates of the CRs were retrieved on June 21, 2024.

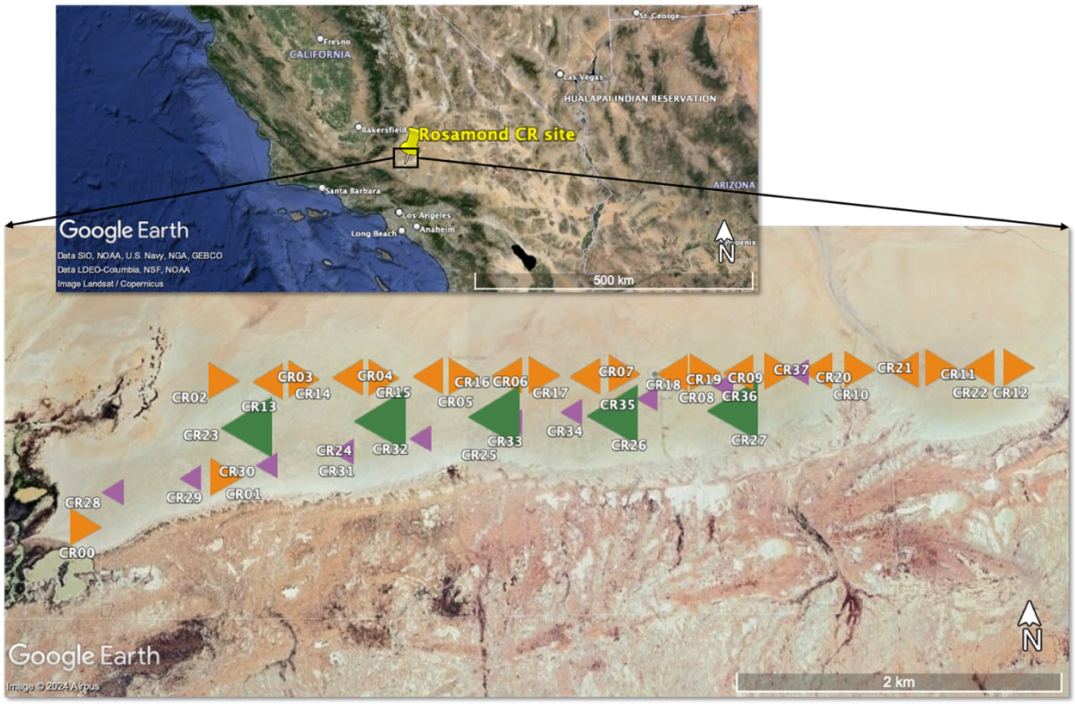

Figure 8. The upper image is a Google Earth overview of the location of the Rosamond Corner Reflector Array (RCRA) site in the Southern California desert. The lower image shows a closer view of the RCRA along the lakebed edge, showing the CR names, alignment, and orientation. The green are the 4.8 m CRs, orange are 2.4 m CRs, and purple are the 0.7 and 0.8 m CRs.

Table 4. Corner Reflectors used for the analysis at the Rosamond site (Data collected 2024-06-21).

CR ID	Latitude (°)	Longitude (°)	Height Above Ellipsoid (m)	Orientation (°)	Elevation angle (°)	Size (m)
0	34.79696932	-118.0965309	660.7852	170.5	12.1	2.4384
1	34.79984857	-118.0869889	661.0341	170.5	8.72	2.4384
2	34.80523758	-118.0873893	660.7954	170	9.3	2.4384
3	34.80533835	-118.0820138	660.9892	171.9	15.67	2.4384
4	34.80541552	-118.0763783	661.1542	176	11.93	2.4384
5	34.80549374	-118.0708034	661.2239	171	11.07	2.4384
6	34.8055848	-118.0652259	661.251	170	10.53	2.4384
7	34.80566749	-118.0596985	661.4004	170	14.7	2.4384
8	34.80575789	-118.0540223	661.5718	170.25	14.53	2.3989
9	34.80581416	-118.0489156	661.4445	175	10.63	2.4384
10	34.80592455	-118.0434141	661.5764	170	14.6	2.4384
11	34.80602488	-118.0377367	661.7005	170	14.6	2.3989
12	34.80607399	-118.0323024	661.9123	169.5	8.1	2.4384
13	34.80519277	-118.0844199	660.9357	347	11.9	2.4384
14	34.80544019	-118.0789226	661.1562	350	16	2.4384
15	34.80552374	-118.0732807	661.3498	350.5	14.2	2.3989
16	34.80554868	-118.0678694	661.283	350	8.03	2.4384
17	34.80555368	-118.062629	661.3207	346	11	2.4384
18	34.80568773	-118.0564286	661.442	346	8.97	2.4384
19	34.80572732	-118.0517599	661.5661	351.25	13.8	2.3989

20	34.80583808	-118.0463583	661.4451	350	10.77	2.4384
21	34.80590046	-118.0403336	661.468	352	8.67	2.4384
22	34.8059963	-118.0351481	661.8095	10.82	16.23	2.4384
23	34.80250461	-118.0858056	661.1992	351.06	21	4.8
24	34.80290963	-118.0766469	661.4273	350.97	20.9	4.8
25	34.80315674	-118.0687807	661.5122	349.69	21	4.8
26	34.8032285	-118.0605827	661.6264	350.66	20.82	4.8
27	34.80351971	-118.0522807	661.6456	349.64	20.93	4.8
28	34.79888394	-118.0948329	661.7209	11.63	14.8	0.8
29	34.79972493	-118.0895139	661.6025	91.5	34	0.7
30	34.80045801	-118.0843115	661.7022	91	33.8	0.7
31	34.80122333	-118.0790955	661.9541	351	16.7	0.7
32	34.80198199	-118.0737945	661.8984	90.5	33.2	0.7
33	34.80291901	-118.0675157	661.9958	354	20	0.7
34	34.80349571	-118.0633953	662.2285	350.54	19.5	0.8
35	34.80426743	-118.0581257	662.1268	91	31.6	0.7
36	34.80501205	-118.0528938	662.0529	92	31.5	0.7
37	34.80577955	-118.0476746	662.2017	351	28.1	0.7

The Oklahoma NISAR Calibration Array is distributed in the northern (Enid), western (Clinton), and southern (Lawton) regions of Oklahoma (Figure 9). Since June 2021, seventeen (17) 2.8 m triangular trihedral CRs have been deployed. Table 5 lists the CRs installed at the Oklahoma sites.

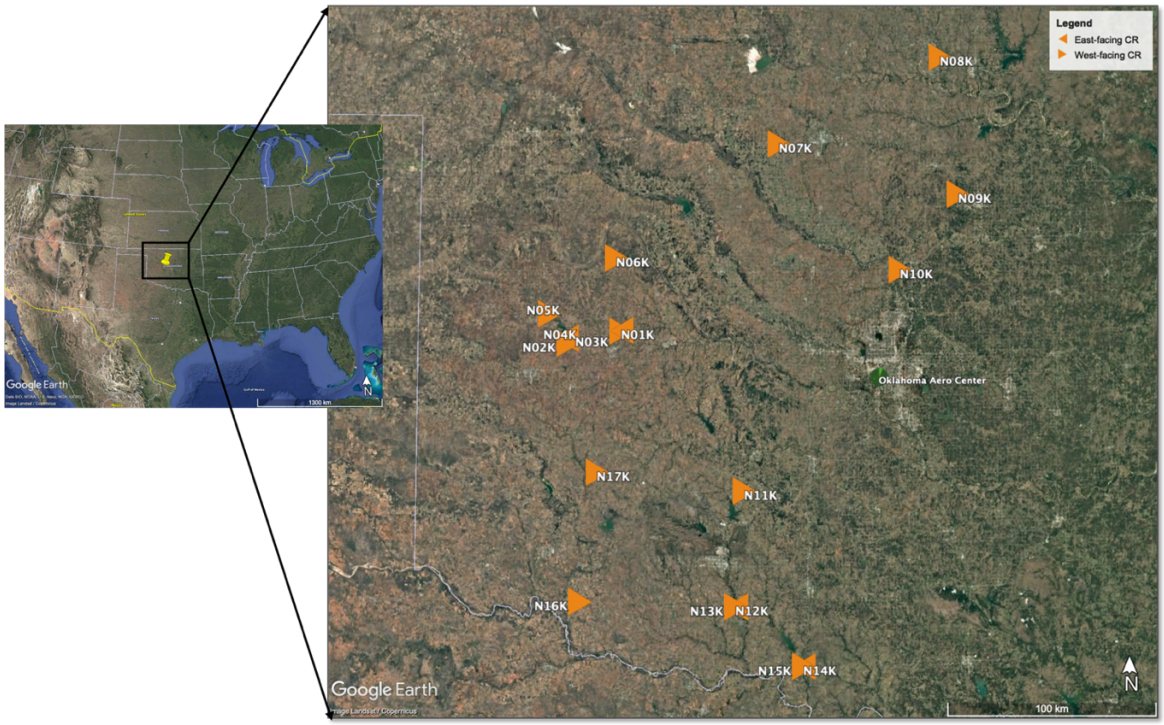

Figure 9. A Google Earth view of the NISAR Calibration array in Oklahoma. The triangles show CR names and distribution at the site.

Table 5. Corner Reflectors used for the analysis at the Oklahoma site (Data collected 2025-09-01).

CR ID	Latitude (°)	Longitude (°)	Height Above Ellipsoid (m)	Orientation (°)	Elevation angle (°)	Size (m)
N01K	35.59190297	-98.93222676	480.1110	359.54	13.97	2.8
N02K	35.53645812	-99.21004167	481.1376	199.23	17.55	2.8
N03K	35.58880703	-98.93568526	479.3595	179.86	14.00	2.8
N04K	35.55705136	-99.21896452	475.6046	4.04	15.25	2.8
N12K	34.42324977	-98.33622366	284.0825	197.97	17.75	2.8
N13K	34.42231663	-98.33661716	283.6386	359.92	13.95	2.8
N14K	34.16798652	-97.98778916	257.6385	181.32	14.25	2.8
N15K	34.16725260	-97.98811293	256.1992	358.82	16.23	2.8

Twenty Spotlight scenes were acquired over the Oklahoma CR sites. Because the Enid, Clinton, and Lawton corner reflector array sites are separated by distances of several hundred kilometers, each Umbra scene covers different CR sites. While the N01K and N03K, N02K and N04K, N12K and N13K, and N14K and N15K pairs are co-located, each pair faces in opposing directions.

4.1. Spatial Resolution

4.1.1. Method

Umbra SAR imagery is designed to deliver sub-meter to meter-scale resolution products depending on the imaging mode.

The spatial resolution of the Umbra imagery was validated using point target analysis tools provided in the GAMMA software, specifically the Single Look Complex (SLC)-based point target analysis command *ptarg_SLC,* which estimates the -3 dB width of the main lobe in range and azimuth for a given corner reflector. The analysis was performed using SICD data generated with the polar format algorithm, that were converted to read in GAMMA SLC format. Assessment of the spatial resolution for Umbra imagery was performed using both the RCRA and Oklahoma corner reflector calibration sites.

The IRF quality parameters, PSLR and ISLR, for Umbra are not provided in the Umbra product guide documentation. Instead, as shown on Figure 10, the reference values for PSLR and ISLR were simulated using the vendor-provided information in the metadata. For an ideal simulated Umbra IRF with uniform (rectangular) weighting, the theoretical PSLR and ISLR are -13.26 dB and -9.7 dB, respectively. We used these reference values for the evaluation.

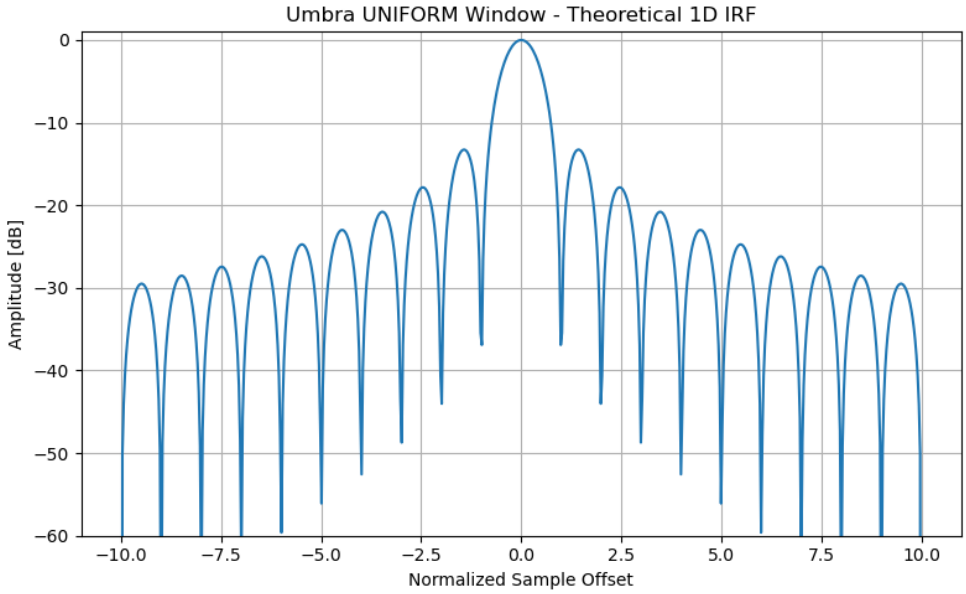

Figure 3. Simulated impulse response using uniform (rectangular) windowing function provided typical Umbra metadata parameters.

4.1.2. Results Compliance

Umbra does not publicly publish formal PSLR/ISLR reference values in its product documentation. For well-focused SAR data processed with uniform weighing, which Umbra used for focusing, theoretical PSLR values are typically on the order of -13 dB. Similarly, ISLR values for high-resolution X-band SAR systems are commonly reported in the range of approximately -10 to -20 dB depending on window functions.

A summary table of IRF analysis results derived from corner reflectors across all analyzed images at Rosamond and Oklahoma is presented in Table 6. In total, 1104 corner reflector image chips were used to compute the summary statistics. The statistical analysis was performed separately for each resolution mode provided by the vendor. The vendor specifies a ground plane impulse response resolution ranging from 0.25 m to 1.0 m in Spotlight mode. The statistical analysis was conducted using all available datasets. As shown in Table 6, the measured PSLR and ISLR values fall within the expected ranges, indicating focusing quality and sidelobe suppression is consistent with other typical X-band SAR systems.

Table 6. Summary table of IRF quality assessment derived from corner reflectors from all analyzed images at the Rosamond and Oklahoma sites. The ground range resolution was estimated by multiplying the slant range resolution by the sine of the incidence angle.

Target Res. [m]	Slant-Range Res. [m]	Ground Range Res. [m]	Azimuth Res. [m]	Range PSLR [dB]	Azimuth PSLR [dB]	Range ISLR [dB]	Azimuth ISLR [dB]
0.25	0.18 ± 0.02	0.26 ± 0.02	0.24 ± 0.02	-13.53 ± 1.26	-14.53 ± 2.3	-12.71 ± 1.63	-14.23 ± 3.06
0.35	0.22 ± 0.05	0.38 ± 0.04	0.33 ± 0.03	-13.20 ± 0.82	-14.28 ± 1.97	-12.33 ± 0.76	-14.01 ± 2.27
0.5	0.30 ± 0.09	0.62 ± 0.07	0.41 ± 0.07	-15.13 ± 2.32	-18.09 ± 3.06	-14.82 ± 2.82	18.39 ± 3.01
1.0	0.61 ± 0.17	1.27 ± 0.15	0.78 ± 0.14	-16.00 ± 2.37	-19.60 ± 3.27	-16.22 ± 3.07	-19.92 ± 3.12

A summary of the spatial resolution assessment is also provided based on the IRF analysis of all images acquired at Rosamond and Oklahoma. For individual image results in the following sections, only the slant-range resolution is reported. For the summary statistics in Table 6, however, the ground range resolution was computed by projecting the slant-range resolution using the sine of the incidence angle, enabling direct comparison with the vendor-provided specifications. Overall, the measured spatial resolution across the dataset is in close agreement with the vendor-provided specifications. This indicates that system performance meets the expected spatial resolution.

Rosamond Corner Reflector Array, CA, USA

A total of 63 images were acquired over the Rosamond site. Four scenes were excluded because the predicted pixel locations of the corner reflectors were significantly offset, affecting multiple corner reflectors across the images. For these 4 scenes, no identifiable corner reflector response was observed near the predicted locations and reliable IRF measurements could not be obtained. The individual image results for Rosemond are shown below in Table 7.

Table 7. Observed spatial resolution, PSLR and ISLR values in azimuth and range directions over Rosamond, CA.

Sat. #	Acquisition Date	Target Res. [m]	Slant-Range Res. [m]	Azimuth Res. [m]	Range PSLR [dB]	Azimuth PSLR [dB]	Range ISLR [dB]	Azimuth ISLR [dB]
04	20240104	0.35	0.23 ± 0.01	0.35 ± 0.03	-12.87 ± 0.20	-12.83 ± 0.58	-12.05 ± 0.14	-12.02 ± 0.25
04	20240818	0.25	0.19 ± 0.02	0.24 ± 0.02	-14.02 ± 1.03	-14.54 ± 1.68	-13.65 ± 0.88	-15.17 ± 2.27
04	20240822	0.25	0.20 ± 0.02	0.25 ± 0.02	-14.33 ± 0.77	-16.07 ± 1.97	-14.10 ± 0.93	-16.88 ± 2.43
05	20240111	0.25	0.14 ± 0.01	0.23 ± 0.02	-11.98 ± 0.59	-14.53 ± 1.44	-11.54 ± 0.56	-14.40 ± 1.47
05	20240820	0.25	0.21 ± 0.02	0.25 ± 0.02	-14.81 ± 1.36	-16.09 ± 1.45	-14.83 ± 0.77	-16.85 ± 1.61
05	20240831	0.25	0.17 ± 0.01	0.26 ± 0.02	-12.87 ± 0.21	-12.46 ± 0.64	-11.43 ± 0.12	-11.16 ± 0.49
05	20240911	0.25	0.20 ± 0.02	0.23 ± 0.01	-14.33 ± 0.83	-15.07 ± 1.36	-13.96 ± 1.11	-15.05 ± 2.33
05	20241014	0.5	0.32 ± 0.02	0.40 ± 0.02	-16.57 ± 1.43	-19.95 ± 1.85	-16.97 ± 1.30	-20.34 ± 1.34
05	20241020	0.5	0.37 ± 0.03	0.42 ± 0.04	-18.18 ± 1.71	-20.95 ± 2.66	-19.18 ± 1.82	-21.32 ± 2.34
05	20241022	0.5	0.29 ± 0.02	0.44 ± 0.06	-13.95 ± 1.37	-18.45 ± 4.61	-13.48 ± 1.23	-17.15 ± 3.57
05	20241023	0.5	0.42 ± 0.00	0.45 ± 0.00	-16.02 ± 0.00	-14.50 ± 0.00	-14.43 ± 0.00	-14.37 ± 0.00
05	20241105	0.5	0.46 ± 0.04	0.42 ± 0.03	-19.61 ± 3.42	-22.16 ± 3.00	-19.91 ± 4.09	-21.86 ± 2.53
05	20241114	0.5	0.18 ± 0.01	0.38 ± 0.03	-12.66 ± 1.17	-17.56 ± 2.79	-11.73 ± 1.31	-16.96 ± 1.91
05	20241116	0.5	0.50 ± 0.04	0.52 ± 0.04	-15.64 ± 1.90	-15.26 ± 1.28	-15.77 ± 2.18	-15.51 ± 1.56
06	20240103	0.35	0.28 ± 0.00	0.34 ± 0.04	-13.61 ± 1.31	-14.84 ± 1.47	-13.12 ± 0.86	-14.83 ± 1.10
06	20240111	0.25	0.19 ± 0.01	0.23 ± 0.01	-12.92 ± 0.60	-14.42 ± 0.82	-12.70 ± 0.71	-14.86 ± 0.67
06	20240902	0.25	0.16 ± 0.01	0.25 ± 0.02	-11.89 ± 0.16	-12.92 ± 0.44	-11.38 ± 0.12	-11.30 ± 0.33
06	20240910	0.25	0.18 ± 0.01	0.25 ± 0.02	-12.50 ± 0.78	-13.12 ± 0.43	-11.62 ± 0.37	-11.66 ± 0.35
06	20240929	0.25	0.20 ± 0.01	0.26 ± 0.02	-12.33 ± 0.26	-12.76 ± 0.45	-11.46 ± 0.14	-11.36 ± 0.39
06	20241001	0.25	0.17 ± 0.01	0.24 ± 0.02	-12.02 ± 0.40	-13.04 ± 0.77	-11.51 ± 0.37	-11.92 ± 0.66
07	20240817	0.25	0.14 ± 0.01	0.24 ± 0.02	-13.33 ± 0.52	-15.53 ± 1.35	-11.98 ± 0.49	-15.78 ± 1.46
07	20240820	0.25	0.19 ± 0.02	0.25 ± 0.02	-14.14 ± 0.71	-15.46 ± 1.74	-13.55 ± 0.59	-16.12 ± 1.99
07	20240903	0.25	0.18 ± 0.01	0.25 ± 0.02	-13.31 ± 0.46	-12.68 ± 0.44	-11.43 ± 0.19	-11.33 ± 0.39
07	20240912	0.25	0.17 ± 0.01	0.25 ± 0.02	-13.24 ± 0.31	-13.13 ± 0.69	-11.51 ± 0.20	-12.03 ± 0.59
07	20240915	0.25	0.19 ± 0.01	0.23 ± 0.02	-16.41 ± 1.44	-19.52 ± 2.99	-17.00 ± 1.72	-20.18 ± 3.11
08	20240818	0.16	0.13 ± 0.01	0.16 ± 0.02	-14.27 ± 0.88	-14.78 ± 3.19	-13.91 ± 1.07	-14.74 ± 3.67
08	20240820	0.25	0.19 ± 0.01	0.24 ± 0.02	-14.04 ± 0.75	-16.12 ± 2.15	-13.41 ± 0.88	-16.63 ± 2.26
08	20240901	0.25	0.14 ± 0.01	0.24 ± 0.02	-13.10 ± 0.16	-12.71 ± 0.51	-11.46 ± 0.12	-11.44 ± 0.45
08	20240902	0.16	0.11 ± 0.01	0.14 ± 0.01	-13.03 ± 0.61	-11.93 ± 0.93	-11.58 ± 0.19	-10.33 ± 1.17
08	20240910	0.25	0.15 ± 0.02	0.21 ± 0.01	-14.62 ± 0.79	-18.13 ± 1.80	-14.14 ± 0.81	-18.86 ± 1.48

08	20240917	0.25	0.17 ± 0.01	0.24 ± 0.01	-13.89 ± 0.54	-15.33 ± 1.40	-12.94 ± 0.44	-15.83 ± 1.36
08	20240928	0.25	0.18 ± 0.01	0.25 ± 0.02	-13.06 ± 0.14	-12.79 ± 0.46	-11.43 ± 0.15	-11.26 ± 0.42
08	20241004	0.25	0.18 ± 0.01	0.25 ± 0.02	-13.32 ± 0.20	-12.69 ± 0.55	-11.71 ± 0.18	-11.80 ± 0.49
08	20241009	0.5	0.34 ± 0.03	0.41 ± 0.03	-16.20 ± 1.82	-20.72 ± 2.13	-17.21 ± 1.45	-21.09 ± 1.59
08	20241018	0.5	0.40 ± 0.02	0.43 ± 0.03	-19.16 ± 2.75	-21.17 ± 2.41	-20.06 ± 2.44	-21.11 ± 2.52
08	20241021	0.5	0.30 ± 0.02	0.45 ± 0.03	-13.87 ± 0.80	-17.28 ± 1.64	-13.19 ± 0.83	-18.11 ± 1.59
09	20241028	0.5	0.16 ± 0.01	0.38 ± 0.02	-13.85 ± 0.88	-17.85 ± 1.68	-12.49 ± 0.90	-18.02 ± 1.68
09	20241122	0.5	0.40 ± 0.00	0.21 ± 0.00	-16.21 ± 0.00	-14.93 ± 0.00	-15.35 ± 0.00	-14.54 ± 0.00
09	20241123	1	0.72 ± 0.07	0.26 ± 0.01	-15.20 ± 0.55	-14.13 ± 1.86	-14.92 ± 1.24	-12.92 ± 1.09
09	20241124	0.5	0.45 ± 0.04	0.18 ± 0.02	-16.25 ± 1.89	-11.70 ± 1.35	-16.78 ± 2.43	-10.58 ± 1.34
05	20250926	1	0.47 ± 0.03	0.75 ± 0.06	-14.19 ± 0.73	-17.81 ± 1.78	-13.44 ± 0.75	-18.91 ± 1.61
05	20250930	1	0.65 ± 0.05	0.77 ± 0.06	-16.69 ± 0.92	-20.44 ± 2.27	-17.15 ± 0.78	-20.88 ± 1.70
05	20251005	0.5	0.26 ± 0.01	0.37 ± 0.03	-14.72 ± 0.71	-18.90 ± 2.36	-14.43 ± 0.76	-19.49 ± 1.78
08	20250926	1	0.74 ± 0.07	0.83 ± 0.05	-19.12 ± 1.78	-22.60 ± 1.88	-20.77 ± 1.59	-22.69 ± 1.37
08	20250928	1	0.76 ± 0.06	0.87 ± 0.07	-17.12 ± 1.79	-19.94 ± 2.19	-18.10 ± 1.62	-20.88 ± 1.72
08	20250930	0.5	0.22 ± 0.02	0.38 ± 0.03	-14.45 ± 1.04	-18.30 ± 1.43	-13.50 ± 1.04	-19.05 ± 1.11
08	20251004	0.5	0.28 ± 0.02	0.38 ± 0.03	-14.78 ± 1.02	-19.00 ± 2.44	-14.73 ± 1.03	-19.48 ± 2.59
09	20250925	1	0.65 ± 0.05	0.80 ± 0.05	-16.44 ± 1.65	-21.34 ± 3.54	-17.46 ± 1.47	-21.47 ± 2.65
09	20250930	0.5	0.36 ± 0.02	0.48 ± 0.03	-14.51 ± 1.11	-16.80 ± 1.88	-14.08 ± 0.72	-17.68 ± 1.80
09	20250930	1	0.36 ± 0.02	0.48 ± 0.03	-14.51 ± 1.11	-16.80 ± 1.88	-14.08 ± 0.72	-17.68 ± 1.80
09	20251001	0.5	0.28 ± 0.02	0.44 ± 0.03	-14.13 ± 0.59	-16.98 ± 1.70	-13.26 ± 0.52	-17.68 ± 1.54
09	20251001	1	0.64 ± 0.04	0.79 ± 0.06	-16.43 ± 1.50	-21.58 ± 2.14	-17.07 ± 1.30	-21.61 ± 1.57
09	20251002	1	0.34 ± 0.02	0.73 ± 0.05	-13.77 ± 0.94	-17.67 ± 2.25	-12.78 ± 0.91	-17.99 ± 2.13
09	20251004	0.5	0.22 ± 0.01	0.37 ± 0.02	-14.27 ± 0.75	-18.62 ± 2.12	-13.44 ± 0.83	-19.11 ± 1.76
10	20250930	0.5	0.79 ± 0.04	0.84 ± 0.06	-18.56 ± 3.00	-21.00 ± 3.38	-19.49 ± 3.23	-21.11 ± 3.25
10	20250930	1	0.79 ± 0.04	0.84 ± 0.06	-18.56 ± 3.00	-21.00 ± 3.38	-19.49 ± 3.23	-21.11 ± 3.25
10	20251001	0.5	0.26 ± 0.02	0.44 ± 0.04	-13.73 ± 0.73	-16.94 ± 1.83	-12.83 ± 0.68	-17.68 ± 1.84
10	20251001	1	0.62 ± 0.04	0.79 ± 0.05	-16.35 ± 1.17	-21.34 ± 2.07	-16.38 ± 1.02	-21.52 ± 1.31
10	20251002	1	0.30 ± 0.02	0.73 ± 0.05	-13.37 ± 0.80	-16.97 ± 2.58	-12.28 ± 0.77	-17.57 ± 2.63
10	20251004	0.5	0.23 ± 0.02	0.38 ± 0.03	-14.54 ± 0.95	-18.74 ± 1.89	-13.83 ± 0.74	-19.44 ± 1.25

4.1.2.2 NISAR Calibration Array, Oklahoma, USA

IRF analysis was performed on 32 of the 33 images acquired over the Oklahoma evaluation site. One image (Scene ID: 1bdad67a-3d5f-4110-ae2e-e8f39f07fe08) was excluded from the analysis because the corner reflector was not visible due to the satellite look direction. The individual image results for Oklahoma are shown below in Table 8.

Table 8. Observed spatial resolution, PSLR and ISLR values in azimuth and range directions over Oklahoma.

Sat. #	Acquisition Date	Target Res. [m]	Scene Center [Lon, Lat]	Slant-Range Res. [m]	Azimuth Res. [m]	Range PSLR [dB]	Azimuth PSLR [dB]	Range ISLR [dB]	Azimuth ISLR [dB]
05	20250906	0.35	-98.936, 35.589	0.26	0.31	-13.39	-12.64	-12.13	-13.66
05	20250910	0.35	-98.936, 35.589	0.18	0.28	-12.71	-21.17	-13.27	-19.51
05	20250924	1	-98.336, 34.423	0.49	0.96	-12.95	-16.76	-12.07	-18.69
05	20250926	1	-98.336, 34.423	0.53	0.75	-14.64	-22.52	-14.68	-22.62
05	20250926	0.5	-98.936, 35.589	0.25	0.51	-13.05	-13.2	-11.55	-11.63
05	20250928	0.5	-97.988, 34.168	0.41	0.38	-18.93	-18.81	-19.24	-19.68
08	20250906	0.35	-98.936, 35.589	0.2	0.35	-13.53	-14.05	-12.01	-13.99
08	20250909	0.35	-99.210, 35.536	0.19	0.3	-11.89	-16.12	-10.96	-17.25

Sat. #	Acquisition Date	Target Res. [m]	Scene Center [Lon, Lat]	Slant-Range Res. [m]	Azimuth Res. [m]	Range PSLR [dB]	Azimuth PSLR [dB]	Range ISLR [dB]	Azimuth ISLR [dB]
08	20250909	0.35	-98.936, 35.589	0.14	0.34	-13.1	-15.4	-11.67	-15.14
08	20250911	0.35	-99.210, 35.536	0.16	0.28	-12.86	-15.21	-11.97	-16.2
08	20250911	0.35	-98.936, 35.589	0.14	0.32	-13.46	-16.61	-11.93	-16.39
08	20250925	1	-97.988, 34.168	0.34	0.46	-12.83	-13.96	-11.99	-12.9
08	20250925	0.5	-98.336, 34.423	0.7	1.02	-13.2	-15.04	-12.39	-14.7
08	20250927	0.5	-98.936, 35.589	0.24	0.43	-11.76	-16.04	-11.2	-16.19
08	20250928	0.5	-97.988, 34.168	0.36	0.41	-15.53	-15.06	-14.9	-15.59
08	20250930	0.5	-98.936, 35.589	0.3	0.5	-12.68	-15.8	-12.6	-16.87
09	20250906	0.35	-98.336, 34.423	0.15	0.35	-12.94	-12.5	-11.53	-10.43
09	20250907	0.35	-98.336, 34.423	0.21	0.34	-13.51	-15.4	-12.55	-15.99
09	20250925	1	-98.336, 34.423	0.77	0.82	-12.96	-13.68	-12.29	-12.99
09	20250926	1	-98.336, 34.423	0.81	1.14	-12.56	-20.43	-12.98	-20.76
09	20250928	0.5	-98.936, 35.589	0.3	0.5	-14.76	-16.55	-13.81	-17.05
09	20250929	0.5	-97.988, 34.168	0.27	0.37	-13.71	-20.02	-13.66	-20.06
10	20250905	0.35	-99.210, 35.536	0.15	0.3	-13.68	-13.39	-12.21	-14.36
10	20250906	0.35	-98.936, 35.589	0.2	0.31	-14.07	-17.4	-13.03	-18.56
10	20250906	0.35	-98.336, 34.423	0.16	0.32	-13.3	-14.04	-11.61	-12.64
10	20250907	0.35	-98.336, 34.423	0.24	0.3	-13.64	-13.48	-12.47	-13.94
10	20250924	1	-98.336, 34.423	0.66	0.99	-13	-13.67	-11.51	-12.56
10	20250926	1	-98.336, 34.423	0.75	0.98	-14.14	-18.49	-13.33	-18.97
10	20250927	0.5	-97.988, 34.168	0.37	0.45	-13.05	-13.52	-11.74	-12.21
10	20250928	0.5	-98.936, 35.589	0.27	0.4	-13.45	-18.68	-13.32	-18.82
10	20250929	1	-98.336, 34.423	0.45	1.28	-13.23	-18.71	-13.52	-18.92
10	20250929	0.5	-98.936, 35.589	0.14	0.5	-12.7	-12.79	-11.34	-11.28

4.2. Geolocation Accuracy

4.2.1. Method

The geolocation accuracy was calculated based on the corner reflectors at the Rosamond and Oklahoma calibration test sites. The assessment of the Umbra images was performed using the GAMMA Remote Sensing software and its SLC point target analysis tool, *ptarg_SLC*. This tool first provides an initial estimate of the corner reflector location and then refines the peak position within a 16 x 16 pixel analysis window centered on that estimate.

However, due to geolocation inaccuracies found in some Umbra images, we found the initial corner reflector location estimated by *ptarg_SLC* could be significantly offset from the true corner reflector position. As a result, the actual corner reflector response was sometimes located outside the 16 x 16 pixel analysis window and could not be properly identified. In such cases, an internally developed Python script was used to search a larger area to accurately determine the peak corner reflector location. The expected SAR image coordinates of corner reflectors were calculated based on satellite orbit (sensor position and velocity) and their known geographic locations and then were compared to the SAR image coordinates of the peak signal locations (Figure 11).

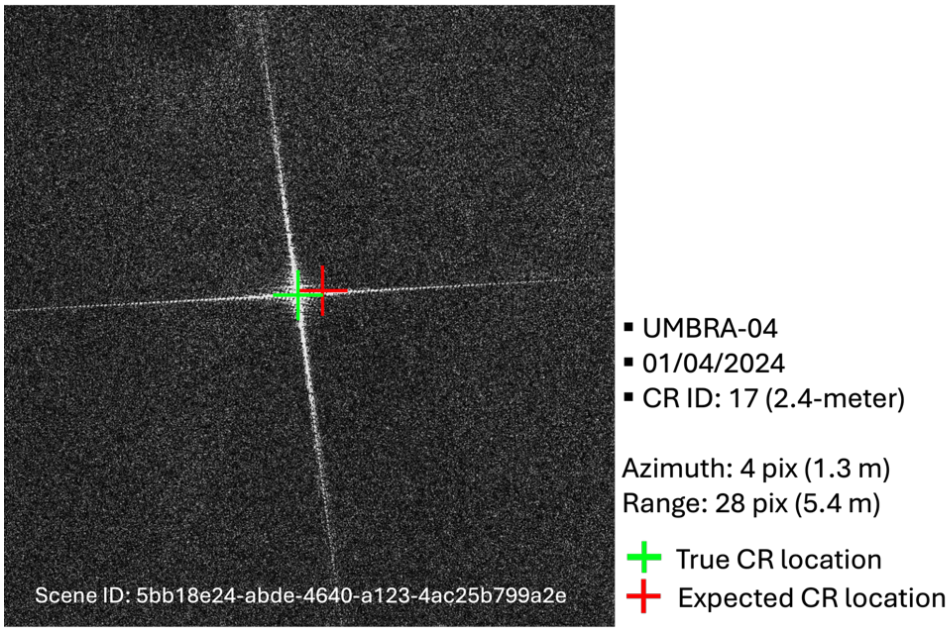

Figure 4. Demonstration of geolocation accuracy assessment. The expected CR location (red) is compared with the observed location in the Umbra SAR image (green). The image chip is from the scene ID [5bb18e24-abde-4640-a123-4ac25b799a2e] over CR17 at the Rosamond site. The figure shows 4- and 28-pixel offsets in azimuth and range directions, respectively, between the expected and observed CR location.

The geolocation errors were measured in range and azimuth direction separately in absolute value, and the absolute location error (ALE) was then calculated using the equation below:

$$ALE = \sqrt{\left(Err_{rg,mean}\right)^2 + \left(Err_{az,mean}\right)^2}$$

4.2.2. Results Compliance

The absolute geolocation accuracy provided in Umbra Product Guide (Umbra, 2025) is 8 m CE90. The geolocation accuracy of the Umbra scenes was evaluated against this specification given by the vendor.

Rosamond Corner Reflector Array, CA, USA

For the Rosamond site, we analyzed 63 Spot mode images to calculate geolocation errors. Table 9 lists the results of the geolocation accuracy analysis for the various Umbra images collected over the Rosamond site.

Table 9. Rosamond geolocation accuracy analysis for Umbra; average and standard deviation of all observed CRs.

Sat. #	Acquisition Date	Target Res.	Range Location Error [m]	Azimuth Location Error [m]	Absolute Location Error [m]
04	20240104	0.35	5.49 ± 0.12	3.12 ± 1.68	6.31 ± 0.84
04	20240818	0.25	5.58 ± 1.39	19.04 ± 9.48	19.84 ± 9.11
04	20240822	0.25	9.48 ± 1.49	20.28 ± 9.75	22.39 ± 8.86
05	20240111	0.25	4.00 ± 0.42	5.89 ± 3.48	7.12 ± 2.89
05	20240820	0.25	2.61 ± 1.83	14.88 ± 8.94	15.11 ± 8.81
05	20240831	0.25	4.24 ± 0.07	2.43 ± 1.50	4.89 ± 0.75
05	20240911	0.25	2.30 ± 1.86	17.83 ± 11.21	17.98 ± 11.12
05	20241014	0.5	5.10 ± 3.15	21.12 ± 11.85	21.73 ± 11.54
05	20241020	0.5	6.94 ± 4.18	25.25 ± 13.54	26.19 ± 13.10
05	20241022	0.5	3.01 ± 1.93	15.29 ± 9.28	15.58 ± 9.11
05	20241023	0.5	55.60 ± 0.00	58.30 ± 0.00	80.56 ± 0.00
05	20241105	0.5	31.14 ± 8.97	31.96 ± 19.66	44.62 ± 15.41
05	20241114	0.5	5.63 ± 0.98	6.75 ± 4.05	8.79 ± 3.17
05	20241116	0.5	8.15 ± 4.30	21.55 ± 14.17	23.04 ± 13.34
06	20240103	0.35	0.95 ± 0.56	9.20 ± 5.06	9.25 ± 5.03
06	20240111	0.25	0.94 ± 0.51	10.03 ± 6.67	10.07 ± 6.64
06	20240902	0.25	4.78 ± 0.08	8.29 ± 1.60	9.57 ± 1.39
06	20240910	0.25	5.67 ± 0.11	11.65 ± 3.72	12.96 ± 3.35
06	20240929	0.25	4.85 ± 0.06	18.88 ± 1.65	19.49 ± 1.60
06	20241001	0.25	5.29 ± 0.23	6.46 ± 4.31	8.35 ± 3.34
07	20240817	0.25	0.76 ± 0.53	8.24 ± 5.17	8.27 ± 5.15
07	20240820	0.25	2.54 ± 1.82	13.31 ± 8.63	13.55 ± 8.48
07	20240903	0.25	4.91 ± 0.06	2.14 ± 1.76	5.36 ± 0.71
07	20240912	0.25	4.25 ± 0.26	5.96 ± 3.86	7.32 ± 3.15
07	20240915	0.25	5.64 ± 3.60	16.71 ± 10.43	17.64 ± 9.95
08	20240818	0.16	2.21 ± 1.22	11.13 ± 6.11	11.35 ± 6.00
08	20240820	0.25	2.78 ± 2.02	14.22 ± 9.22	14.49 ± 9.06
08	20240901	0.25	1.79 ± 0.07	3.66 ± 2.13	4.07 ± 1.91
08	20240902	0.16	6.88 ± 0.10	2.05 ± 1.75	7.18 ± 0.51
08	20240910	0.25	3.24 ± 1.98	13.74 ± 8.68	14.12 ± 8.46
08	20240917	0.25	6.51 ± 1.62	12.59 ± 8.82	14.17 ± 7.87
08	20240928	0.25	4.49 ± 0.05	1.78 ± 1.52	4.83 ± 0.56
08	20241004	0.25	1.98 ± 0.30	6.43 ± 4.76	6.73 ± 4.55
08	20241009	0.5	6.37 ± 4.62	21.73 ± 13.42	22.64 ± 12.94
08	20241018	0.5	9.75 ± 6.36	30.91 ± 16.14	32.41 ± 15.51
08	20241021	0.5	5.40 ± 2.52	12.24 ± 8.59	13.38 ± 7.92
09	20241028	0.5	2.46 ± 0.49	4.04 ± 2.36	4.73 ± 2.03
09	20241122	0.5	24.14 ± 0.00	12.83 ± 0.00	27.34 ± 0.00
09	20241123	1	10.33 ± 1.99	13.52 ± 8.33	17.01 ± 6.73
09	20241124	0.5	14.83 ± 1.04	9.17 ± 6.59	17.44 ± 3.58
05	20250926	1	5.10 ± 1.37	9.38 ± 6.09	10.68 ± 5.39
05	20250930	1	4.52 ± 3.40	17.92 ± 12.64	18.48 ± 12.28
05	20251005	0.5	8.14 ± 1.97	9.81 ± 5.72	12.75 ± 4.58
08	20250926	1	6.88 ± 5.19	20.16 ± 12.95	21.30 ± 12.37
08	20250928	1	10.84 ± 6.32	23.76 ± 15.91	26.12 ± 14.71
08	20250930	0.5	6.93 ± 1.41	11.45 ± 8.03	13.38 ± 6.91

Sat. #	Acquisition Date	Target Res.	Range Location Error [m]	Azimuth Location Error [m]	Absolute Location Error [m]
08	20251004	0.5	2.26 ± 1.40	11.50 ± 7.29	11.72 ± 7.16
09	20250925	1	5.83 ± 4.43	19.14 ± 12.75	20.01 ± 12.26
09	20250930	0.5	8.09 ± 3.02	18.24 ± 10.81	19.95 ± 9.96
09	20250930	1	9.84 ± 7.76	31.01 ± 17.42	32.53 ± 16.77
09	20251001	0.5	2.60 ± 1.77	12.08 ± 7.55	12.36 ± 7.39
09	20251001	1	5.12 ± 3.31	22.90 ± 16.26	23.47 ± 15.88
09	20251002	1	1.19 ± 0.53	8.08 ± 4.54	8.17 ± 4.49
09	20251004	0.5	3.47 ± 1.86	10.65 ± 6.88	11.20 ± 6.57
10	20250930	0.5	6.28 ± 3.88	20.85 ± 11.72	21.78 ± 11.28
10	20250930	1	9.23 ± 6.42	31.53 ± 18.90	32.85 ± 18.23
10	20251001	0.5	4.03 ± 1.43	10.65 ± 6.32	11.39 ± 5.93
10	20251001	1	4.69 ± 3.31	19.36 ± 10.92	19.92 ± 10.64
10	20251002	1	3.00 ± 0.35	2.89 ± 1.88	4.17 ± 1.33
10	20251004	0.5	4.80 ± 2.24	12.31 ± 8.01	13.21 ± 7.51

Based on a statistical analysis of geolocation accuracy using 1,069 corner reflector image chips from 63 scenes acquired at the Rosamond site in 2024 and 2025, the observed geolocation errors were 5.31 m ± 4.58 m in the range direction and 14.76 m ± 13.53 m in the azimuth direction. At the Rosamond site, approximately 32% of the samples exhibit an ALE below 8 m, indicating that only a third of the CR reference samples meet the expected geolocation accuracy.

NISAR Calibration Array, Oklahoma, USA

For the Oklahoma site, we analyzed 33 Spotlight mode images to calculate geolocation errors. Table 10 presents the results of the geolocation accuracy analysis for various Umbra satellites over the Oklahoma site.

Based on a statistical analysis of geolocation accuracy using 35 corner reflector image chips from 33 scenes acquired at the Oklahoma site in 2025, the observed geolocation errors were 5.36 m ± 3.98 m in the range direction and 10.99 m ± 18.75 m in the azimuth direction. At the Oklahoma site, approximately 63% of the images fell within the expected ALE of 8 m, however some rather extreme geolocation errors of over 50 m were observed.

Table 10. Geolocation accuracy analysis over the Oklahoma site; the values are calculated from a single CR observed within a scene.

Sat. #	Acquisition Date	Target Res.	Scene Center [Lon, Lat]	Range Location Error [m]	Azimuth Location Error [m]	Absolute Location Error [m]
05	20250906	0.35	-98.936, 35.589	-8.25	-5.04	9.67
05	20250910	0.35	-98.936, 35.589	-4.63	-6.89	8.30
05	20250924	1	-98.336, 34.423	-3.28	-2.8	4.31
05	20250926	1	-98.336, 34.423	1.16	-3.99	4.16
05	20250926	0.5	-98.936, 35.589	2.89	-4.34	5.21
05	20250928	0.5	-97.988, 34.168	2.37	-29.09	29.19

Sat. #	Acquisition Date	Target Res.	Scene Center [Lon, Lat]	Range Location Error [m]	Azimuth Location Error [m]	Absolute Location Error [m]
08	20250906	0.35	-98.936, 35.589	-6.59	3.01	7.24
08	20250909	0.35	-99.210, 35.536	8.22	12.25	14.75
08	20250909	0.35	-98.936, 35.589	4.21	5.27	6.75
08	20250911	0.35	-99.210, 35.536	7.06	2.07	7.36
08	20250911	0.35	-98.936, 35.589	-5.39	3.99	6.71
08	20250925	1	-97.988, 34.168	-5.46	3.7	6.60
08	20250925	0.5	-98.336, 34.423	-1.07	-50.32	50.33
08	20250927	0.5	-98.936, 35.589	5.77	54.2	54.51
08	20250928	0.5	-97.988, 34.168	10.22	8.29	13.16
08	20250930	0.5	-98.936, 35.589	5.62	-0.22	5.62
09	20250906	0.35	-98.336, 34.423	1.64	5.33	5.58
09	20250907	0.35	-98.336, 34.423	4.18	5.3	6.75
09	20250925	1	-98.336, 34.423	16.19	59.48	61.64
09	20250926	1	-98.336, 34.423	12.92	94.26	95.14
09	20250928	0.5	-98.936, 35.589	-7.03	8.1	10.73
09	20250929	0.5	-97.988, 34.168	-3.38	4.54	5.66
10	20250905	0.35	-99.210, 35.536	7.15	10.99	13.11
10	20250906	0.35	-98.936, 35.589	2.81	4.32	5.15
10	20250906	0.35	-98.336, 34.423	2.34	6.52	6.93
10	20250907	0.35	-98.336, 34.423	5.27	8.77	10.23
10	20250924	1	-98.336, 34.423	12.35	59.68	60.94
10	20250926	1	-98.336, 34.423	-18.78	69.17	71.67
10	20250927	0.5	-97.988, 34.168	2.26	2.56	3.41
10	20250928	0.5	-98.936, 35.589	2.88	3.03	4.18
10	20250929	1	-98.336, 34.423	-3.82	2.12	4.37
10	20250929	0.5	-98.936, 35.589	-1.3	2.87	3.15

4.2.3. Summary of Geolocation Accuracy Assessment

In Figure 12 we show the distribution of geolocation errors in the range and azimuth directions derived from the corner reflector measurements at the Rosamond and Oklahoma evaluation sites. Each point in Figure 12 represents the geolocation error estimated from image chips collected over individual corner reflectors. The results show that the azimuth directional (x-axis) errors are significantly larger than those in the range direction.

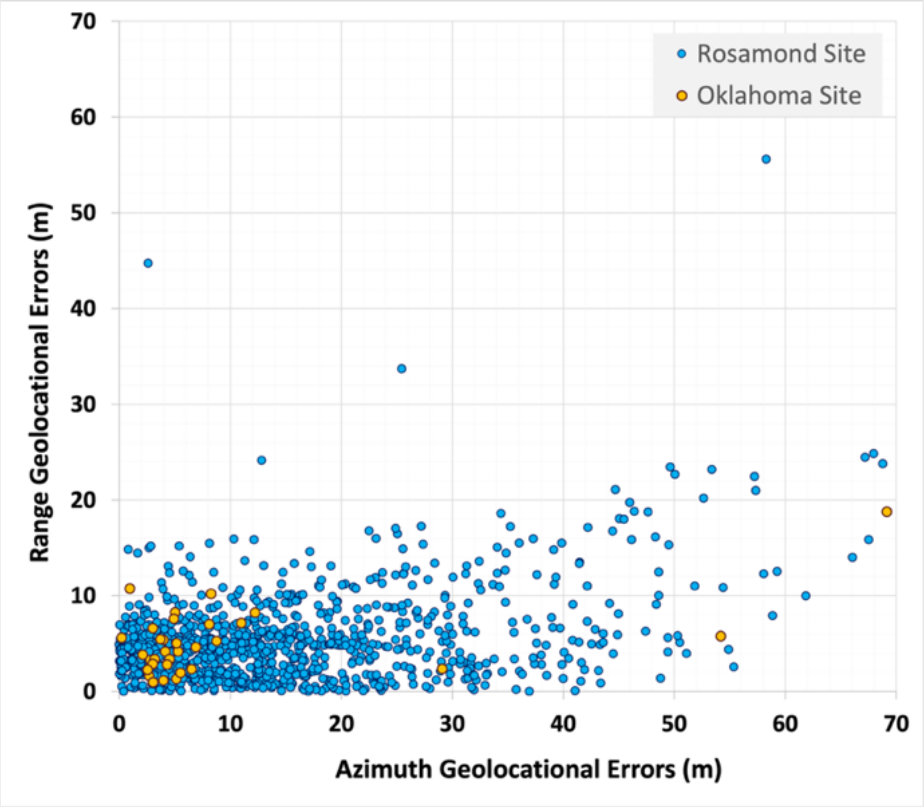

Figure 5. Geolocation errors in range and azimuth directions derived from corner reflectors at Rosamond and Oklahoma sites.

Based on a statistical analysis of geolocation accuracy using 1104 corner reflector image chips collected from 63 scenes acquired at the Rosamond site in 2024 and 2025, and 33 scenes acquired at the Oklahoma site in 2025, the observed geolocation errors were 5.30 m ± 4.56 m in the range direction and 14.64 m ± 13.73 m in the azimuth direction. The geolocation accuracy in the range direction falls within the 8 m expected geolocation error range. However, the observed azimuth-direction geolocation accuracy was found to be over 5 m beyond the expected error range. Geolocation accuracy was also evaluated using the absolute location error (ALE) computed from all corner reflector image chips that take into account both range and azimuth directions. The mean and standard deviation of ALE from all 1104 samples was 16.37 ± 13.56, indicating that the overall positioning performance does not meet the expected accuracy of 8 m.

References

Doerry, A. W. (2014). *Reflectors for SAR Performance Testing–second edition* (No. SAND--2014-0882). Sandia National Laboratories (SNL-NM), Albuquerque, NM (United States).

European Space Agency (ESA), 2015. *Sentinel-1A TOPS Radiometric Calibration Refinement*. ESA Technical Report. Available online: https://sentinels.copernicus.eu/documents/

247904/2142675/Sentinel-1A_TOPS_Radiometric_Calibration_Refinement.pdf

Gelaro, R., McCarty, W., Suárez, M. J., Todling, R., Molod, A., Takacs, L., Randles, C. A., Darmenov, A., Bosilovich, M. G., Reichle, R., & others. (2017). *The modern-era retrospective analysis for research and applications, version 2 (MERRA-2*). Journal of Climate, 30(14), 5419–5454.

Li, X.-M., & Lehner, S. (2013). *Algorithm for sea surface wind retrieval from TerraSAR-X and TanDEM-X data.* IEEE Transactions on Geoscience and Remote Sensing*, 52*(5), 2928–2939.

National Geospatial-Intelligence Agency. (2023). *Sensor Independent Complex Data (SICD), Volume 1: Design & Implementation Description Document (Version 1.4.0)*. National Geospatial-Intelligence Agency.

Marinkovic, P., Ketelaar, G., van Leijen, F., & Hanssen, R. (2007). *InSAR quality control: Analysis of five years of corner reflector time series.* Proceedings of the Fringe 2007 Workshop (ESA SP-649), Frascati, Italy, 26–30.

Schmidt, K., Schwerdt, M., & Miranda, N. (2021, March). *Inter-comparability of radiometric performance between Sentinel-1A and Sentinel-1B*. In EUSAR 2021; 13th European Conference on Synthetic Aperture Radar (pp. 1-4). VDE.

Schwerdt, M., Schmidt, K., Klenk, P., Tous Ramon, N., Rudolf, D., Raab, S., ... & Zink, M. (2018). *Radiometric performance of the TerraSAR-X mission over more than ten years of operation*. Remote Sensing, 10(5), 754.

Ulaby, F., Dobson, M. C., & Álvarez-Pérez, J. L. (2019). *Handbook of radar scattering statistics for terrain*. Artech House.

Umbra Lab Inc, *Umbra SAR system specifications*. Available at: https://help.umbra.space/product-guide/umbra-sar-system-specifications (accessed March 23, 2026)

Umbra Lab Inc. (2025). *Umbra Product Guide*. Online document https://help.umbra.space/product-guide. Accessed 31 July 2025.

Umbra Lab Inc. (2026). *Umbra Calibration Activity*. Umbra internal proprietary document. Revised 01/28/2026 .

Van Zyl, J. J., & Zebker, H. A. (1990). Imaging radar polarimetry. *Progress in Electromagnetics Research*, *3*, 277-326.

APPENDIX A

Table A1. List of Umbra acquisitions used for the radiometric assessment.

Test Area	Satellite Number	Imaging Mode	Look Direction	Polarization	Acquisition Date	Incidence Angle
Rosamond, California	UMBRA_04	ASCENDING	LEFT	VV	20240818	49.37
	UMBRA_04	ASCENDING	LEFT	VV	20240822	50.58
	UMBRA_05	ASCENDING	LEFT	VV	20240820	54.55
	UMBRA_05	ASCENDING	LEFT	VV	20240831	41.57
	UMBRA_06	ASCENDING	LEFT	VV	20240902	39.76
	UMBRA_07	ASCENDING	LEFT	VV	20240817	32.26
	UMBRA_07	ASCENDING	LEFT	VV	20240903	44.55
	UMBRA_07	ASCENDING	LEFT	VV	20240912	42.62
	UMBRA_08	ASCENDING	LEFT	VV	20240901	33.87
Doldrums	UMBRA_05	ASCENDING	LEFT	HH	20250908	26.16
	UMBRA_05	ASCENDING	LEFT	HH	20250904	26.32
	UMBRA_05	ASCENDING	LEFT	HH	20250909	26.33
	UMBRA_05	ASCENDING	LEFT	HH	20250906	34.05
	UMBRA_05	ASCENDING	LEFT	HH	20250902	34.46
	UMBRA_05	ASCENDING	RIGHT	HH	20250903	28.82
	UMBRA_05	DESCENDING	LEFT	HH	20250830	25.72
	UMBRA_05	DESCENDING	RIGHT	HH	20250907	25.29
	UMBRA_05	DESCENDING	RIGHT	HH	20250905	33.9
	UMBRA_08	ASCENDING	LEFT	HH	20250906	25.86
	UMBRA_08	ASCENDING	LEFT	HH	20250827	28.67
	UMBRA_08	ASCENDING	LEFT	VV	20250901	34.17
	UMBRA_08	ASCENDING	RIGHT	HH	20250908	28.59
	UMBRA_08	DESCENDING	RIGHT	HH	20250829	21.37
	UMBRA_08	DESCENDING	RIGHT	HH	20250908	28.32
	UMBRA_08	DESCENDING	RIGHT	VV	20250903	29.2
	UMBRA_08	DESCENDING	RIGHT	VV	20250909	29.26
	UMBRA_09	ASCENDING	LEFT	HH	20250906	21.56
	UMBRA_09	ASCENDING	LEFT	HH	20250830	27.71
	UMBRA_09	ASCENDING	LEFT	HH	20250909	28.4
	UMBRA_09	ASCENDING	LEFT	HH	20250829	33.93
	UMBRA_09	ASCENDING	LEFT	HH	20250831	34.89
	UMBRA_09	ASCENDING	RIGHT	HH	20250904	23.47
	UMBRA_09	ASCENDING	RIGHT	HH	20250906	34.03
	UMBRA_09	ASCENDING	RIGHT	HH	20250827	34.04
	UMBRA_09	DESCENDING	LEFT	HH	20250903	26.76
	UMBRA_09	DESCENDING	RIGHT	HH	20250828	17.33
	UMBRA_09	DESCENDING	RIGHT	HH	20250829	17.67
	UMBRA_10	ASCENDING	LEFT	HH	20250906	24.06
	UMBRA_10	ASCENDING	LEFT	HH	20250830	29.9
	UMBRA_10	ASCENDING	LEFT	HH	20250909	30.66
	UMBRA_10	ASCENDING	LEFT	HH	20250829	34.15
	UMBRA_10	ASCENDING	RIGHT	HH	20250904	20.62
	UMBRA_10	ASCENDING	RIGHT	HH	20250827	32.3
	UMBRA_10	ASCENDING	RIGHT	HH	20250906	34.09
	UMBRA_10	DESCENDING	LEFT	HH	20250903	24.28
	UMBRA_10	DESCENDING	RIGHT	HH	20250829	20.02

Test Area	Satellite Number	Imaging Mode	Look Direction	Polarization	Acquisition Date	Incidence Angle
	UMBRA_10	DESCENDING	RIGHT	HH	20250828	20.13
	UMBRA_10	DESCENDING	RIGHT	HH	20250905	20.45
	UMBRA_10	DESCENDING	RIGHT	VV	20250906	34.39
Amazon	UMBRA_05	ASCENDING	LEFT	HH	20250829	33.75
	UMBRA_05	ASCENDING	LEFT	VV	20250901	34.31
	UMBRA_05	ASCENDING	RIGHT	HH	20250828	29.77
	UMBRA_05	ASCENDING	RIGHT	HH	20250829	34.15
	UMBRA_05	DESCENDING	LEFT	HH	20250901	24.41
	UMBRA_05	DESCENDING	LEFT	HH	20250829	32.27
	UMBRA_05	DESCENDING	LEFT	VV	20250829	25.47
	UMBRA_05	DESCENDING	RIGHT	HH	20250902	27.87
	UMBRA_08	ASCENDING	LEFT	HH	20250829	23.74
	UMBRA_08	ASCENDING	LEFT	HH	20250818	33.95
	UMBRA_08	ASCENDING	RIGHT	HH	20250904	15.39
	UMBRA_08	ASCENDING	RIGHT	HH	20250830	18.75
	UMBRA_08	ASCENDING	RIGHT	HH	20250904	19.7
	UMBRA_08	ASCENDING	RIGHT	HH	20250828	24.67
	UMBRA_08	ASCENDING	RIGHT	HH	20250901	31.75
	UMBRA_08	ASCENDING	RIGHT	HH	20250902	32.92
	UMBRA_08	DESCENDING	LEFT	HH	20250905	20.07
	UMBRA_08	DESCENDING	LEFT	HH	20250830	24.72
	UMBRA_08	DESCENDING	LEFT	HH	20250831	25.7
	UMBRA_08	DESCENDING	LEFT	HH	20250817	34.08
	UMBRA_08	DESCENDING	RIGHT	HH	20250901	24.2
	UMBRA_08	DESCENDING	RIGHT	HH	20250820	24.54
	UMBRA_08	DESCENDING	RIGHT	HH	20250911	29.8
	UMBRA_09	ASCENDING	LEFT	HH	20250903	28.59
	UMBRA_09	ASCENDING	LEFT	HH	20250820	28.67
	UMBRA_09	ASCENDING	LEFT	HH	20250903	33.09
	UMBRA_09	ASCENDING	RIGHT	HH	20250828	29.71
	UMBRA_09	ASCENDING	RIGHT	HH	20250831	30.41
	UMBRA_09	ASCENDING	RIGHT	HH	20250817	31.08
	UMBRA_09	DESCENDING	LEFT	HH	20250816	33.94
	UMBRA_10	ASCENDING	LEFT	HH	20250820	30.64
	UMBRA_10	ASCENDING	LEFT	HH	20250831	33.95
	UMBRA_10	ASCENDING	LEFT	HH	20250903	34.11
	UMBRA_10	ASCENDING	RIGHT	HH	20250828	27.39
	UMBRA_10	ASCENDING	RIGHT	HH	20250831	28.16
	UMBRA_10	ASCENDING	RIGHT	HH	20250817	28.99
	UMBRA_10	DESCENDING	LEFT	HH	20250829	22.93
	UMBRA_10	DESCENDING	LEFT	HH	20250830	26.78
	UMBRA_10	DESCENDING	RIGHT	HH	20250831	20.18
	UMBRA_10	DESCENDING	RIGHT	HH	20250819	27.31

Table A2. List of Umbra acquisitions used for the geometric assessment.

Test Area	Satellite Number	Imaging Mode	Look Direction	Polarization	Acquisition Date	Target Res.	Incidence Angle
Rosamond	UMBRA_04	DESCENDING	RIGHT	HH	20240104	0.35	39.60
	UMBRA_04	ASCENDING	LEFT	VV	20240818	0.25	49.37
	UMBRA_04	ASCENDING	LEFT	VV	20240822	0.25	50.58
	UMBRA_05	DESCENDING	RIGHT	HH	20240111	0.25	32.13

Test Area	Satellite Number	Imaging Mode	Look Direction	Polarization	Acquisition Date	Target Res.	Incidence Angle
	UMBRA_05	ASCENDING	LEFT	VV	20240820	0.25	54.55
	UMBRA_05	ASCENDING	LEFT	VV	20240831	0.25	41.57
	UMBRA_05	ASCENDING	LEFT	HH	20240911	0.25	48.92
	UMBRA_05	ASCENDING	RIGHT	HH	20241014	0.5	38.89
	UMBRA_05	ASCENDING	RIGHT	HH	20241020	0.5	43.59
	UMBRA_05	DESCENDING	LEFT	VV	20241022	0.5	33.96
	UMBRA_05	ASCENDING	LEFT	HH	20241023	0.5	67.62
	UMBRA_05	DESCENDING	RIGHT	HH	20241105	0.5	61.08
	UMBRA_05	DESCENDING	LEFT	HH	20241114	0.5	19.31
	UMBRA_05	ASCENDING	LEFT	HH	20241116	0.5	75.59
	UMBRA_05	ASCENDING	RIGHT	HH	20241121	0.5	73.60
	UMBRA_05	ASCENDING	RIGHT	HH	20241126	0.5	73.77
	UMBRA_06	DESCENDING	RIGHT	HH	20240103	0.35	48.78
	UMBRA_06	DESCENDING	RIGHT	HH	20240111	0.25	45.22
	UMBRA_06	ASCENDING	LEFT	VV	20240902	0.25	39.76
	UMBRA_06	ASCENDING	LEFT	HH	20240910	0.25	47.07
	UMBRA_06	ASCENDING	LEFT	HH	20240929	0.25	54.22
	UMBRA_06	ASCENDING	LEFT	HH	20241001	0.25	42.80
	UMBRA_07	ASCENDING	LEFT	VV	20240817	0.25	32.26
	UMBRA_07	DESCENDING	RIGHT	VV	20240820	0.25	46.93
	UMBRA_07	ASCENDING	LEFT	VV	20240903	0.25	44.55
	UMBRA_07	ASCENDING	LEFT	VV	20240912	0.25	42.62
	UMBRA_07	DESCENDING	RIGHT	HH	20240915	0.25	48.77
	UMBRA_08	ASCENDING	LEFT	HH	20240818	0.16	53.06
	UMBRA_08	DESCENDING	RIGHT	VV	20240820	0.25	48.70
	UMBRA_08	ASCENDING	LEFT	VV	20240901	0.25	33.87
	UMBRA_08	ASCENDING	LEFT	HH	20240902	0.16	53.08
	UMBRA_08	DESCENDING	RIGHT	HH	20240910	0.25	34.65
	UMBRA_08	DESCENDING	RIGHT	HH	20240917	0.25	42.08
	UMBRA_08	ASCENDING	LEFT	HH	20240928	0.25	46.65
	UMBRA_08	ASCENDING	LEFT	HH	20241004	0.25	48.67
	UMBRA_08	ASCENDING	LEFT	VV	20241009	0.5	39.54
	UMBRA_08	ASCENDING	RIGHT	HH	20241018	0.5	48.35
	UMBRA_08	DESCENDING	RIGHT	VV	20241021	0.5	36.31
	UMBRA_08	DESCENDING	RIGHT	HH	20241023	0.5	79.46
	UMBRA_09	ASCENDING	RIGHT	HH	20241028	0.5	18.91
	UMBRA_09	DESCENDING	RIGHT	HH	20241122	0.5	63.99
	UMBRA_09	ASCENDING	RIGHT	HH	20241123	1	57.52
	UMBRA_09	ASCENDING	LEFT	HH	20241124	0.5	73.60
	UMBRA_05	ASCENDING	RIGHT	HH	20250926	1	26.30
	UMBRA_05	ASCENDING	LEFT	HH	20250930	1	37.68
	UMBRA_05	ASCENDING	RIGHT	HH	20251005	0.5	29.87
	UMBRA_08	DESCENDING	RIGHT	HH	20250926	1	45.22
	UMBRA_08	ASCENDING	LEFT	HH	20250928	1	47.48
	UMBRA_08	ASCENDING	LEFT	HH	20250930	0.5	24.92
	UMBRA_08	ASCENDING	RIGHT	HH	20251004	0.5	32.66
	UMBRA_09	DESCENDING	RIGHT	HH	20250925	1	40.67
	UMBRA_09	ASCENDING	RIGHT	HH	20250930	1	47.65
	UMBRA_09	ASCENDING	RIGHT	HH	20250930	0.5	43.72
	UMBRA_09	ASCENDING	RIGHT	HH	20251001	1	38.11
	UMBRA_09	ASCENDING	RIGHT	HH	20251001	0.5	32.45
	UMBRA_09	ASCENDING	RIGHT	HH	20251002	1	19.18

Test Area	Satellite Number	Imaging Mode	Look Direction	Polarization	Acquisition Date	Target Res.	Incidence Angle
	UMBRA_09	ASCENDING	LEFT	HH	20251004	0.5	25.55
	UMBRA_10	ASCENDING	RIGHT	HH	20250930	1	47.80
	UMBRA_10	ASCENDING	RIGHT	HH	20250930	0.5	43.50
	UMBRA_10	ASCENDING	RIGHT	HH	20251001	1	36.42
	UMBRA_10	ASCENDING	RIGHT	HH	20251001	0.5	30.68
	UMBRA_10	ASCENDING	RIGHT	HH	20251002	1	16.66
	UMBRA_10	ASCENDING	LEFT	HH	20251004	0.5	27.31
Oklahoma	UMBRA_05	DESCENDING	LEFT	HH	20250924	1	26.68
	UMBRA_05	ASCENDING	LEFT	HH	20250926	1	33.22
	UMBRA_05	ASCENDING	LEFT	VV	20250926	0.5	28.09
	UMBRA_05	ASCENDING	LEFT	VV	20250928	0.5	45.43
	UMBRA_08	DESCENDING	LEFT	VV	20250925	1	40.40
	UMBRA_08	ASCENDING	RIGHT	HH	20250927	1	41.27
	UMBRA_08	DESCENDING	LEFT	VV	20250925	0.5	42.98
	UMBRA_08	ASCENDING	RIGHT	VV	20250927	0.5	30.17
	UMBRA_08	DESCENDING	RIGHT	VV	20250928	0.5	42.55
	UMBRA_08	DESCENDING	RIGHT	VV	20250930	0.5	34.05
	UMBRA_09	DESCENDING	RIGHT	VV	20250925	1	55.88
	UMBRA_09	ASCENDING	RIGHT	VV	20250926	1	55.93
	UMBRA_09	ASCENDING	RIGHT	VV	20250928	0.5	34.45
	UMBRA_09	ASCENDING	RIGHT	HH	20250929	0.5	30.89
	UMBRA_10	DESCENDING	RIGHT	VV	20250924	1	48.78
	UMBRA_10	ASCENDING	RIGHT	VV	20250926	1	55.79
	UMBRA_10	ASCENDING	RIGHT	HH	20250929	1	26.14
	UMBRA_10	ASCENDING	RIGHT	VV	20250927	0.5	45.88
	UMBRA_10	ASCENDING	RIGHT	VV	20250928	0.5	34.26
	UMBRA_10	ASCENDING	RIGHT	VV	20250929	0.5	16.56